

Accepted Manuscript

Structure-based design and *in vivo* anti-arthritis activity evaluation of a potent dipeptidyl cyclopropyl nitrile inhibitor of cathepsin C

Brice Korkmaz, Adam Lesner, Magdalena Wysocka, Artur Gieldon, Maria Håkansson, Francis Gauthier, Derek T. Logan, Dieter Jenne, Conni Lauritzen, John Pedersen

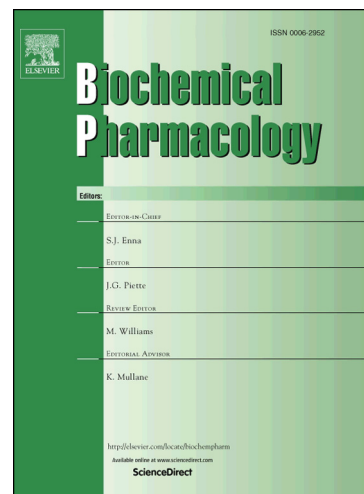
PII: S0006-2952(19)30141-8
DOI: <https://doi.org/10.1016/j.bcp.2019.04.006>
Reference: BCP 13489

To appear in: *Biochemical Pharmacology*

Received Date: 22 February 2019
Accepted Date: 7 April 2019

Please cite this article as: B. Korkmaz, A. Lesner, M. Wysocka, A. Gieldon, M. Håkansson, F. Gauthier, D.T. Logan, D. Jenne, C. Lauritzen, J. Pedersen, Structure-based design and *in vivo* anti-arthritis activity evaluation of a potent dipeptidyl cyclopropyl nitrile inhibitor of cathepsin C, *Biochemical Pharmacology* (2019), doi: <https://doi.org/10.1016/j.bcp.2019.04.006>

This is a PDF file of an unedited manuscript that has been accepted for publication. As a service to our customers we are providing this early version of the manuscript. The manuscript will undergo copyediting, typesetting, and review of the resulting proof before it is published in its final form. Please note that during the production process errors may be discovered which could affect the content, and all legal disclaimers that apply to the journal pertain.



Structure-based design and *in vivo* anti-arthritic activity evaluation of a potent dipeptidyl cyclopropyl nitrile inhibitor of cathepsin C

Brice Korkmaz^{1,2}, Adam Lesner³, Magdalena Wysocka³, Artur Gieldon³, Maria Håkansson⁴, Francis Gauthier^{1,2}, Derek T. Logan⁴, Dieter Jenne^{5,6}, Conni Lauritzen⁷ and John Pedersen⁷

¹INSERM, UMR 1100, “Centre d’Etude des Pathologies Respiratoires”, 37032 Tours, France;

²Université de Tours, 37032 Tours, France; ³Faculty of Chemistry, University of Gdansk, 80-308 Gdansk, Poland; ⁴SARomics Biostructures, 223 63 Lund, Sweden; ⁵Comprehensive Pneumology Center, Institute of Lung Biology and Disease, German Center for Lung Research (DZL), 81377 Munich, Germany; ⁶Max Planck Institute of Neurobiology, 82152 Planegg-Martinsried, Germany; ⁷Neuprozyme Therapeutics A/S, 2970 Hörsholm, Denmark.

***Corresponding author:** Brice Korkmaz (PhD)

INSERM U-1100 “Centre d’Etude des Pathologies Respiratoires (CEPR)”,

Université François Rabelais, Faculté de Médecine

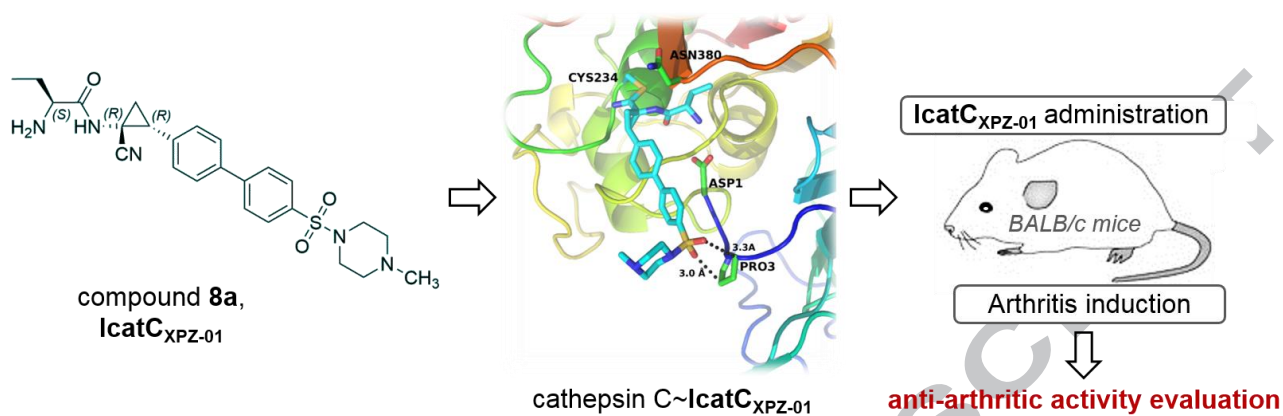
10 Bld. Tonnellé, 37032, Tours, France

e-mail: brice.korkmaz@inserm.fr

Tel: 0033 2 47 36 63 86

Fax: 0033 2 47 36 60 46

Graphical abstract



Abstract

Cathepsin C (CatC) is a dipeptidyl-exopeptidase which activates neutrophil serine protease precursors (elastase, proteinase 3, cathepsin G and NSP4) by removing their N-terminal propeptide in bone marrow cells at the promyelocytic stage of neutrophil differentiation. The resulting active proteases are implicated in chronic inflammatory and autoimmune diseases. Hence, inhibition of CatC represents a therapeutic strategy to suppress excessive protease activities in various neutrophil mediated diseases. We designed and synthesized a series of dipeptidyl cyclopropyl nitrile compounds as putative CatC inhibitors. One compound, **IcatC_{XPZ-01}** ((*S*)-2-amino-N-((1*R*,2*R*)-1-cyano-2-(4'-(4-methylpiperazin-1-ylsulfonyl)biphenyl-4-yl)cyclopropyl)butanamide)) was identified as a potent inhibitor of both human and rodent CatC. In mice, pharmacokinetic studies revealed that **IcatC_{XPZ-01}** accumulated in the bone marrow reaching levels suitable for CatC inhibition. Subcutaneous administration of **IcatC_{XPZ-01}** in a monoclonal anti-collagen antibody induced mouse model of rheumatoid arthritis resulted in statistically significant anti-arthritis activity with persistent decrease in arthritis scores and paw thickness.

Keywords: cathepsin C, cysteine protease, neutrophil, serine protease, inhibitor.

Abbreviations: CAIA, collagen antibody-induced arthritis; Cat, cathepsin; CYP450, cytochromes P450; DTT, dithiothreitol; FRET, fluorescence resonance energy transfer; hERG, human ether-a-go-go-related gene; HPFC, high-performance flash chromatography; HPLC, high performance liquid chromatography; HRMS, high resolution mass spectrometry; IC₅₀, half maximal inhibitory concentration; LPS, lipopolysaccharide; mAb, monoclonal antibody; NE, neutrophil elastase; NSP, neutrophil serine protease; PR3, proteinase 3; PLS, Papillon-Lefèvre syndrome; pNA, *para*-nitroaniline; RT, room temperature.

1. Introduction

Dipeptidyl peptidase I (EC 3.4.14.1), also called cathepsin C (CatC), is a papain family lysosomal cysteine peptidase.¹⁻³ CatC removes dipeptides from the N-terminal end of peptides and proteins with relatively large specificity.⁴ CatC is a key protease in the processing and maturation of granule-associated serine proteases of immune cell lineages² including the lymphocyte granzymes, mast cell chymase and the neutrophil-associated serine proteases (neutrophil elastase (NE), proteinase 3 (PR3), cathepsin G (CatG)⁵⁻⁶ and NSP4⁷). All four neutrophil serine proteases (NSPs) are synthesized and activated during the promyelocyte stage of neutrophil differentiation in the bone marrow and are stored mainly in primary granules in the cytoplasm of neutrophils until they are released.⁸ The removal of N-terminal dipeptides by CatC converts zymogens into active proteases⁵⁻⁶ (**Figure 1**) following conformation changes.⁹ Once activated, unopposed NSPs can cause tissue damage and promote inflammation in pathological situations.¹⁰⁻¹¹

Genetic mutations in the CatC gene (gene symbol: *CTSC*) is responsible for Papillon-Lefèvre syndrome¹² (PLS, OMIM: 245000)¹³⁻¹⁴, a rare disease affecting 1-4 people per million.¹⁵⁻¹⁶ PLS is characterized by severe periodontitis and diffuse transgradient palmo-plantar keratoderma.¹⁷ CatC deficiency results in almost complete elimination of NSPs in blood neutrophils.^{6-7, 18-20} We recently obtained the same results *in vitro* and *in vivo* after a prolonged pharmacological inhibition of CatC.^{18,20} Continuous pharmacological blockade of CatC activity is supposed to lower the NSP load of circulating neutrophils in patients suffering from chronic inflammatory diseases, including cystic fibrosis, bronchiectasis, alpha-1 antitrypsin deficiency and autoimmune diseases especially ANCA-associated vasculitis.^{2, 10, 21} CatC inhibition may also help fighting rheumatoid arthritis as suggested by the observations in CatC^{-/-} mice that are protected against acute arthritis in response to active collagen-type II immunization.^{5, 22}

CatC itself is synthesized as an inactive zymogen bearing a removable internal propeptide.²³⁻²⁴ Evidence has been provided that recombinant CatC zymogen *in vitro* can be activated by CatL and CatS but not autocatalytically.²³ Proteolytically active mature CatC, characterized by its tetrameric structure, consists of four homo-subunits.²⁵⁻²⁷ Each subunit contains an N-terminal fragment (the exclusion domain), a heavy chain and a light chain.^{25, 27} The two latter adopt the papain fold containing the active site. The exclusion domain, the specific structural determinant of CatC, confers CatC its exopeptidase specificity by blocking substrate access beyond the S2 subsite²⁵, according to the nomenclature of Schechter and Berger²⁸ and allowing the Asp1 residue (conserved in all known CatC sequences) to interact with the free amino group of the substrate N-terminal residues²⁷ excluding arginine or lysine. The presence of a proline at P1 or P1', or a P1 isoleucine also precludes substrate hydrolysis by CatC.⁴ CatC that optimally functions at a slightly acidic pH²⁹ is activated by chloride anions in a pH dependent manner.³⁰

We and others have previously designed and developed CatC inhibitors.³¹⁻³⁶ Nitrile-based compounds with three chemical classes of nitrile (cyanamides, aryl or heteroaryl nitriles and amino- or amidoacetonitriles), differing in their electrophilic effects are the most investigated group of inhibitors of CatC.^{2, 32} Amidoacetonitrile-based inhibitors are dipeptides with a nitrile warhead allowing covalent bonding with the cysteine residue (Cys234) of the CatC active site. However, initially developed dipeptidyl nitrile compounds derived from Abu-Bip-CN containing an Abu at P2 and biphenyl (Bip) at P1 (**Figure 2A**) are not stable in plasma due to the rapid hydrolysis of their amide bond.³¹⁻³³ Stabilization of the peptide bond can be obtained through the substitution of the N-terminal amino acid with an amino acid displaying a piperidine or cyclohexyl ring as side chain^{32, 37} (**Figure 2B**). Another strategy to enhance the metabolic stability is the insertion of a 1,1-cyclopropyl amino nitrile moiety in

P1³⁸⁻³⁹ (**Figure 2C**). However, the rigidification of the backbone by cyclopropyl strongly reduces the inhibitory potency of these inhibitors.^{33, 40}

In this work, we have designed and synthesized a novel series of dipeptidyl cyclopropyl nitrile compounds as putative CatC inhibitors with characteristics suitable for *in vivo* use. Structure-activity relationships analysis of crystallized inhibitors in complex with CatC and molecular docking trials were used to characterize the interaction of inhibitors with CatC to optimize efficacy at very low-dose. **IcatC_{XPZ-01}**, a potent and cell-permeable compound ((*S*)-2-amino-N-((1*R*,2*R*)-1-cyano-2-(4'-(4-methylpiperazin-1-ylsulfonyl)biphenyl-4-yl)cyclopropyl)butanamide)) (**Figure 2D**), which displayed an excellent PK-profile leading to high and sustained concentration in the bone marrow, was further evaluated in a mouse model of rheumatoid arthritis induced by anti-collagen antibodies.

2. Materials and methods

2.1. Chemical synthesis of CatC inhibitors

CatC inhibitors were synthesized by PepTech Corporation (Burlington, Massachusetts, USA). The purity of all synthesized compounds was determined by HPLC and LCMS (PepTech Corporation (Burlington, Massachusetts, USA)). The purity of all tested compounds was $\geq 95\%$. Calculated and mass spectrometry determined masses of compounds **1-14** are shown in Table 1.

2.1.1. Chemical synthesis of compound **8a** (**IcatC_{XPZ-01}**) and compound **8b**

(*S*)-2-amino-N-((1*R*,2*R*)-1-cyano-2-(4'-(4-methylpiperazin-1-ylsulfonyl)biphenyl-4-yl)cyclopropyl)butanamide (compound **8a**, **IcatC_{XPZ-01}**) and (*S*)-2-amino-N-((1*S*,2*S*)-1-cyano-2-(4'-(4-methylpiperazin-1-ylsulfonyl)biphenyl-4-yl)cyclopropyl)butanamide (compound **8b**).

N'-(4-bromobenzylidene)-4-methylbenzenesulfonohydrazide (**II**).

To a solution of 4-bromobenzaldehyde (85.1 g, 0.46 mol) in MeOH (1 L) p-toluenesulfonyl hydrazide (98.6 g, 0.53 mol) was added at room temperature (RT) (**Figure 3**). The reaction was stirred for 30 min, then cooled to 0 °C. The precipitate was collected by filtration and washed with cooled MeOH (50 mL × 2). The solid was dried in an oven to afford N'-(4-bromobenzylidene)-4-methylbenzenesulfonohydrazide (**II**) (150.3 g, yield 92%). LC-MS: 354.1 (M+1).

(1*R*,2*R* and 1*S*,2*S*)-methyl-2-(4-bromophenyl)-1-(tert-butyloxycarbonylamino)cyclopropanecarboxylate (**IIIa** and **IIIb**).

A solution of N'-(4-bromobenzylidene)-4-methylbenzenesulfonohydrazide (56.4 g, 0.16 mol) in THF (1 L) was kept at -78 °C. To the solution dropwise n-Butyllithium (64 mL, 0.16 mol) was added. The reaction was stirred for 1 h at -78 °C, and the solvent was removed under vacuum. To the residue was added a mixture of methyl 2-(tert-butyloxycarbonylamino)acrylate (**I**) (32.2 g, 0.16 mol), benzyltriethylammonium chloride (0.91 g, 4 mmol), and catalyst ClFeTPP (0.56 g, 0.4 mmol) in toluene (1 L). The reaction was stirred for 4 days at 50 °C under N₂ protection. The solvent was removed under vacuum and the residue was partitioned between dichloromethane (500 mL) and water (500 mL). The organic layer was collected, and the water layer was extracted with CH₂Cl₂ (500 mL × 2). The organic phases were combined, dried over anhydrous Na₂SO₄, and concentrated. The crude product was purified by HPFC (PE:EA=10:1) to afford a mixture of (1*R*,2*R*)- (**IIIa**) and (1*S*,2*S*)-methyl-2-(4-bromophenyl)-1-(tert-butoxycarbonyl- amino)cyclopropanecarboxylate (**IIIb**) (29.1 g, yield 49%). LC-MS: 371.2 (M+1).

1-Methyl-4-[4-(4,4,5,5-tetramethyl-1,3,2-dioxaborolan-2-yl)phenylsulfonyl]piperazine (**2**).

To a mixture of 1-(4-bromophenyl sulfonyl)-4-methylpiperazine (**1**) (20 g, 62.6 mmol), pinacolatodiboron (11 g, 62.6 mmol), and potassium carbonate (17.8 g, 0.13 mol) in toluene Pd(PPh₃)₄ (3 g) was added (1 L) under nitrogen protection. The mixture was heated under reflux overnight. After cooling to RT, the solvent was removed under vacuum. To the residue were added water (500 mL) and EA (500 mL). The organic phase was collected, and the water phase was extracted with EA (500 mL ×

2). The organic phases were combined, dried over anhydrous sodium sulfate and concentrated to afford **2** (15.1 g, yield 65%). LC-MS: 367.2 (M+I).

(1*R*,2*R*) and (1*S*,2*S*)-methyl 1-(tert-butyloxycarbonylamino)-2-[4'-(4-methyl-piperazin-1-yl-sulfonyl)biphenyl-4-yl]cyclopropanecarboxylate (**3a** and **3b**).

To a mixture of **2** (15 g, 40.9 mol), **IIIa** and **IIIb** (15.1 g, 40.9 mmol) and sodium carbonate aqueous solution (8.67 g, 2 M) in 1,4-dioxane (1 L) PdCl₂(dppf)₂ (2 g) was added under nitrogen protection. The mixture was refluxed overnight. After cooling to RT, the solvent was removed under vacuum. To the residue were added water (500 mL) and EA (500 mL). The organic phase was collected, and the water phase was extracted with EA (500 mL × 2). The organic phases were combined, dried over anhydrous sodium sulfate, and concentrated. The crude product was purified by HPFC (AE /PE as eluent) to afford the **3a** and **3b** mixture (12.9 g, yield 60%). LC- MS: 530.2 (M +I).

(1*R*,2*R*) and (1*S*,2*S*)-methyl-1-amino-2-[4'-(4-methylpiperazin-1-yl-sulfonyl)-biphenyl-4-yl]-cyclopropanecarboxylate (**4**).

To a solution of **3a** and **3b** (2.5 g, 4.7 mmol) in THF (30 mL) 100 mL of aqueous 6 N HCl was added. The mixture was stirred for 4 h at 40 °C, then adjusted to pH 8 with sat. NaHCO₃. The mixture was extracted with EA (200 mL × 3). The organic layers were separated, dried over anhydrous sodium sulfate, and concentrated to afford **4** quantitatively.

(1*R*,2*R*)-methyl-(*S*)-2-(tert-butyloxycarbonylamino)butanamido)-2-(4'-(4-methylpiperazin-1-ylsulfonyl)biphenyl-4-yl)cyclopropanecarboxylate (**5a**) (1*S*,2*S*)-methyl-((*S*)-2-(tert-butyloxycarbonylamino)butanamido)-2-(4'-(4-methyl-piperazin-1-ylsulfonyl)biphenyl-4-yl)cyclopropanecarboxylate (**5b**).

To a solution of Boc-Abu-OH (2.35 g, 9.4 mmol) and NMM (1.77 g, 18.8 mmol) in CH₂Cl₂ (50 mL) at 0 °C ethyl chloroformate (1.03 g, 9.4 mmol) was added. The reaction was stirred for 1 h at 0 °C, and a solution of **4** (2.03 g, 4.7 mmol) in CH₂Cl₂ (10 mL) was added. The reaction was allowed

to warm to RT and stirred overnight. It was poured into 100 mL of water and extracted with dichloromethane (100 mL). The CH₂Cl₂ layer was separated, and the aqueous phase was extracted with dichloromethane (100 mL × 2) and EA (100 mL × 2). The combined organic extract was dried over anhydrous Na₂SO₄ and concentrated under vacuum. The residue was purified by HPFC (ethyl acetate petroleum ether as eluent) to yield a mixture of stereoisomers, which was separated by chiral-HPLC (ChiralPak AD 20 μm, 5×50 cm column temperature 25 °C, detection wavelength 210 nm and 254 nm Flow Rate 70 mL/min Mobile Phase A:Hex 0.1% HOAc ,Mobile Phase B: IPrOH 0.1% HOAc, analysis time 40 min) to afford **5a** (t_R 6.9 min 700 mg) and **5b** (t_R 14.1 min, 650 mg). LC-MS: 615.3 (M+1).

Tert-butyloxycarbonylamino-(*S*)-1-((1*R*,2*R*)-1-carbamoyl-2-(4'-(4-methylpiperazin-1-yl-sulfonyl)biphenyl-4-yl)cyclopropylamino)-1-oxobutan-2-ylcarbamate (**6a**) and Tert-butyloxycarbonylamino-(*S*)-1-((1*S*,2*S*)-1-carbamoyl-2-(4'-(4-methylpiperazin-1-yl-sulfonyl)biphenyl-4-yl)cyclopropylamino)-1-oxobutan-2-ylcarbamate (**6b**).

To a solution of **5a** (0.7 g, 1.1 mmol) in THF (20 mL) and water (20 mL) LiOH×H₂O (0.25 g, 5.5 mmol) was added. The reaction was stirred for 3 h at RT. It was adjusted to pH 3 with aqueous 1 N HCl and extracted with EA (100 mL × 3). The combined extract was dried over anhydrous Na₂SO₄ and concentrated under vacuum. The residue was dissolved in CH₂Cl₂ (50 mL), and NMM (0.33 g, 3.3 mmol) was added. After cooling the solution to 0 °C, ethyl chloroformate (0.24 g, 2.2 mmol) was injected into the reaction mixture. The reaction was stirred for 1 h at 0 °C, and the mixture was poured into a flask with 200 mL of ammonia. The reaction was stirred overnight at RT. The mixture was extracted with CH₂Cl₂ (200 mL × 3) and EA (200 mL × 3). The organic phases were collected, dried over anhydrous Na₂SO₄, and concentrated to afford **6a** (550 mg, 81%). LC-MS: 600.2 (M+H).

To a solution of **5b** (0.65 g, 1.0 mmol) in THF (20 mL) and water (20 mL) LiOH×H₂O (0.25 g, 5.5 mmol) was added. The reaction was stirred for 3 h at RT. It was adjusted to pH 3 with aqueous 1 N HCl and extracted with EA (100 mL × 3). The combined extract was dried over anhydrous

Na₂SO₄ and concentrated under vacuum. The residue was dissolved in CH₂Cl₂ (50 mL) and NMM (0.33 g, 3.3 mmol) was added. After cooling the solution to 0 °C, ethyl chloroformate (0.24 g, 2.2 mmol) was injected into the reaction mixture. The reaction was stirred for 1 h at 0 °C, and the mixture was poured into a flask with 200 mL of ammonia. The reaction was stirred overnight at RT. The mixture was extracted with CH₂Cl₂ (200 mL × 3) and EA (200 mL × 3). The organic phases were collected, dried over anhydrous Na₂SO₄, and concentrated to afford **6b** (520 mg, 82%). LC-MS: 600.3 (M+H).

To a solution of **6a** (550 mg, 0.92 mmol) in DMF (10 mL) cyanuric chloride (0.50 g, 2.75 mmol) was added. The reaction was stirred for 4 h at RT. Solvent was removed under vacuum, and the residue was partitioned between water (30 mL) and EA (60 mL). The organic layer was dried over anhydrous Na₂SO₄ and concentrated under vacuum. The crude product was purified by HPFC (EA) to afford (Boc-compound **8a**) (150 mg). Boc-compound **8a** (150 mg, 0.26 mmol) was treated with excess HCOOH (10 mL) for 4 h at RT. The solution was slowly added into a mixture of NaHCO₃ in water and ice with stirring. After neutralization, the mixture was extracted with EA (200 mL × 3) and CH₂Cl₂ (200 mL × 3). The combined organic extract was dried over anhydrous Na₂SO₄, and concentrated to yield compound **8a** (60 mg). LC-MS: 482.1 (M+H)/calculated mass: 481.6.

¹H NMR (CDCl₃, 300 MHz) δ: 7.81 (d, J - 8.4 Hz, 2H, Ph), 7.68 (d, J - 8.4 Hz, 2H, Ph), 7.54 (d+s, J = 8.1 Hz, 3H, Ph+CONH), 7.34 (d, J = 8.1 Hz, 2H, Ph), 3.19 (m, 1H, COCH), 3.07 (m, 5H, NCH₂+PhCH), 2.51 (m, 4H, NCH₂), 2.28 (s, 3H, NCH₃), 2.09 (m, 1H, cyclopropane-CHz), 1.84 (m, 1H, cyclopropane-CH₂), 1.48 (m, 2H, CH₂), 0.63 (t, J - 7.2 Hz, 3H, CH₃).

To a solution of **6b** (520 mg, 0.87 mmol) in DMF (10 mL) cyanuric chloride (0.50 g, 2.75 mmol) was added. The reaction was stirred for 4 h at RT. The solvent was removed under vacuum, and the residue was partitioned between water (30 mL) and EA (60 mL). The organic layer was dried over anhydrous Na₂SO₄ and concentrated under vacuum. The crude product was purified by HPFC (EA) to afford Boc-compound **8b** (120 mg). Boc-compound **8b** (120 mg, 0.21 mmol) was treated with excess HCOOH (10 mL) for 4 h at RT. The solution was slowly added into a mixture of NaHCO₃ in

water and ice with stirring. After neutralization, the mixture was extracted with EA (200 ml \times 3) and dichloromethane (200 ml \times 3). The combined organic extract was dried over anhydrous Na₂SO₄, and concentrated to yield compound **8b** (98 mg). LC-MS: 482.1 (M+H)/calculated mass: 481.6.

¹H NMR (DMSO-d₆, 300 MHz) δ : 7.90 (d, J = 8.4 Hz, 2H, Ph), 7.78 (d, J = 8.4 Hz, 2H, Ph), 7.66 (d, J = 8.1 Hz, 2H, Ph), 7.34 (d, J = 8.4 Hz, 2H, Ph), 3.10 (t, J = 9.0 Hz, 1H, COCH), 2.91 (m, 4H, NCH₂), 2.84 (m, 1H, PhCH), 2.36 (m, 4H, NCH₂), 2.13 (s, 3H, NCH₃), 1.99 (m, 2H, cyclopropane-CH₂), 1.09 (m, 1H, CH₂), 0.97 (m, 1H, CH₂), 0.37 (t, J = 8.0 Hz, 3H, CH₃).

2.1.2. Spectroscopic data of synthesized CatC inhibitors

Compound **1**, (S)-N-((S)-2-([1,1'-biphenyl]-4-yl)-1-cyanoethyl)-2-aminobutanamide.

(127 mg, 33% yield). LC-MS: 308.1(M+1)/calculated mass: 307.4. ¹H NMR (CDCl₃, 300 MHz) δ : 7.26-7.62 (m, 9H, Ph), 8.52 (br, 2H, NH₂), 8.18 (br, 1H, NH), 4.98 (m, 1H, CH), 3.27 (m, 1H, CH), 3.21-3.01 (m 2H CH₂), 1.84 (br, 2H, CH₂), 0.87 (br, 3H, CH₃).

Compound **2**, (S)-2-amino-N-((S)-1-cyano-2-(4'-fluoro-[1,1'-biphenyl]-4-yl)ethyl)butanamide.

(61 mg, 63% yield). LC-MS: 326.1 (M+H)/calculated mass: 325.5. ¹H NMR (CDCl₃, 300 MHz) δ : 7.13-7.65 (m, 8H, Ph), 8.76 (br, 2H, NH₂), 8.20 (br, 1H, NH), 4.87 (m, 1H, CH), 3.23 (m, 1H, CH), 3.27-3.01 (m 2H CH₂), 1.88 (br, 2H, CH₂), 0.85 (br, 3H, CH₃).

Compound **3**, (S)-2-amino-N-((S)-1-cyano-2-(4'-(trifluoromethyl)-[1,1'-biphenyl]-4-yl)ethyl)butanamide.

(49 mg, 44 % yield). LC-MS: 376.1 (M+H)/calculated mass: 375.4. ¹H NMR (CDCl₃, 300 MHz) δ : 7.28-7.74 (m, 8H, Ph), 8.81 (br, 2H, NH₂), 8.10 (br, 1H, NH), 4.85 (m, 1H, CH), 3.21 (m, 1H, CH), 3.27-3.01 (m 2H CH₂), 1.81 (br, 2H, CH₂), 0.82 (br, 3H, CH₃).

Compound **4a**, (S)-2-amino-N-((1R,2R)-1-cyano-2-(4'-fluorobiphenyl-4-yl)cyclopropyl)butanamide.

(62 mg, 68%). LC-MS: 338.1 (M+1)/calculated mass: 337.4. ¹H NMR (DMSO-d₆, 300 MHz) δ : 7.25-7.68 (m, 8H, Ph), 3.08 (m, 1H, COCH), 3.05 (t, J = 6.4 Hz, 1H, PhCH), 1.97 (d, J = 9.0 Hz, 2H, cyclopropane-CH₂), 1.10 (m, 2H, CH₂), 0.57 (t, J = 7.8 Hz, 3H, CH₃).

Compound **4b**, (S)-2-amino-N-((1S,2S)-1-cyano-2-(4'-fluorobiphenyl-4-yl)cyclopropyl)butanamide.

(68 mg, 75%). LC-MS: 338.1 (M+1)/calculated mass: 337.4. ¹H NMR (DMSO-d₆, 300 MHz) δ : 7.25-7.68 (m, 8H, Ph), 3.80 (t, J = 9.1 Hz, 1H, COCH), 3.05 (t, J = 6.0 Hz, 1H, PhCH), 1.95 (m, 2H, cyclopropane-CH₂), 0.95-1.19 (m, 2H, CH₂), 0.36 (m, J = 7.4 Hz, 3H, CH₃).

Compound **5a**, (S)-2-amino-N-((1R,2R)-1-cyano-2-(4'-(trifluoromethyl)biphenyl-4-yl)cyclopropyl)butanamide.

(70 mg, 74%). LC-MS: 388.1 (M+1)/calculated mass: 387.4. ¹H NMR (DMSO-d₆, 300 MHz) δ : 7.33-7.88 (m, 8H, Ph), 3.09 (t, J = 9.3 Hz, 1H, COCH), 2.92 (t, J = 6.5 Hz, 1H, PhCH), 1.97 (d, J = 9.0 Hz, 2H, cyclopropane-CH₂), 1.10 (m, 2H, CH₂), 0.47 (t, J = 7.5 Hz, 3H, CH₃).

Compound **5b**, (S)-2-amino-N-((1S,2S)-1-cyano-2-(4'-(trifluoromethyl)biphenyl-4-yl)cyclopropyl)butanamide.

(72 mg, 75%). LC-MS: 388.1 (M+1)/calculated mass: 387.4. ¹H NMR (DMSO-d₆, 300 MHz) δ : 7.33-7.88 (m, 8H, Ph), 3.10 (t, J = 9.0 Hz, 1H, COCH), 2.86 (t, J = 6.3 Hz, 1H, PhCH), 1.98 (m, 2H, cyclopropane-CH₂), 0.93-1.18 (m, 2H, CH₂), 0.38 (m, J = 7.6 Hz, 3H, CH₃).

Compound **6a**, (S)-2-amino-N-((1R,2R)-1-cyano-2-(4'-(4-methylpiperazin-1-yl)biphenyl-4-yl)cyclopropyl)butanamide.

(88 mg, 73% yield). LC-MS: 418.2 [M+H]⁺/calculated mass: 417.5. ¹H NMR (DMSO-d₆, 300 MHz) δ : 7.49 (d, J = 8.1 Hz, 4H, Ph), 7.22 (d, J = 8.4 Hz, 2H, Ph), 7.00 (d, J = 8.7 Hz, 2H, Ph), 3.17 (br, 4H, NCH₂), 3.03 (m, 1H, COCH), 2.95 (m, 1H, PhCH), 2.46 (br, 4H, NCH₂), 2.22 (s, 3H, NCH₃), 1.96 (m, 2H, cyclopropane-CH₂), 1.19 (m, 2H, CH₂), 0.62 (t, J = 7.1 Hz, 3H, CH₃).

Compound **6b**, (S)-2-amino-N-((1S,2S)-1-cyano-2-(4'-(4-methylpiperazin-1-yl)biphenyl-4-yl)cyclopropyl)butanamide.

(32 mg, 31% yield). LC-MS: 418.2 $[M+H]^+$ /calculated mass: 417.5. 1H NMR (DMSO- d_6 , 300 MHz): δ 7.48 (d, J = 8.4 Hz, 4H, Ph), 7.22 (d, J = 8.1 Hz, 2H, Ph), 7.00 (d, J = 8.7 Hz, 2H, Ph), 3.17 (br, 4H, NCHi), 3.08 (m, 1H, COCH), 2.93 (m, 1H, PhCH), 2.47 (br, 4H, NCH₂), 2.22 (s, 3H, NCH₃), 1.99 (m, 1H, cyclopropane-CHa), 1.87 (m, 1H, cyclopropane-CH₂), 1.15 (m, 2H, CH₂), 0.36 (t, J = 7.2 Hz, 3H, CH₃).

Compound **7a**, (*S*)-2-amino-*N*-((1*R*,2*R*)-1-cyano-2-(4-(2-(4-methylpiperazin-1-yl)-[1,2,4]triazolo[1,5-*a*]pyridin-6-yl)phenyl)cyclopropyl)butanamide.

(150 mg, 46%). LC-MS: 459.3 (M+1)/calculated mass: 458.6. 1H NMR (CDCl₃, 300 MHz) δ : 8.53 (s, 1H, NH), 7.62-7.46 (m, 5H, Ph+CH), 7.34 (d, J = 8.1 Hz, 2H, Ph), 3.70 (t, J = 4.8 Hz, 4H, NCH₂), 3.21 (m, 1H, CH), 3.10 (m, 1H, CH), 2.58 (t, J = 5.0 Hz, 4H, NCH₂), 2.39 (s, 3H, NCH₃), 2.10 (m, 1H, cyclopropane-CH₂), 1.84 (m, 1H, cyclopropane-CH₂), 1.27 (m, 2H, CH₂), 0.70 (t, J = 7.6 Hz, 3H, CH₃).

Compound **7b**, (*S*)-2-amino-*N*-((1*S*,2*S*)-1-cyano-2-(4-(2-(4-methylpiperazin-1-yl)-[1,2,4]triazolo[1,5-*a*]pyridin-6-yl)phenyl)cyclopropyl)butanamide.

(80 mg, 35%). LC-MS: 459.3 (M+1)/calculated mass: 458.6. 1H NMR (CDCl₃, 300 MHz) δ : 8.55 (s, 1H, NH), 7.63 (d, J = 9.0 Hz, 1H, CH), 7.55-7.47 (m, 4H, Ph+CH), 7.31 (d, J = 8.1 Hz, 2H, Ph), 3.70 (t, J = 5.0 Hz, 4H, NCH₂), 3.16 (m, 1H, CH), 3.05 (m, 1H, CH), 2.59 (t, J = 4.8 Hz, 4H, NCH₂), 2.39 (s, 3H, NCH₃), 2.15 (m, 1H, cyclopropane-CH₂), 1.85 (m, 1H, cyclopropane-CH₂), 1.75-1.38 (m, 2H, CH₂), 0.84 (t, J = 7.5 Hz, 3H, CH₃).

Compound **9a**, 1-amino-*N*-((1*R*,2*R*)-1-cyano-2-(4'-((4-methylpiperazin-1-yl)sulfonyl)-[1,1'-biphenyl]-4-yl)cyclopropyl)cyclohexane-1-carboxamide.

(118 mg, 31%). 1H NMR (CDCl₃, 300 MHz) δ : 7.99 (s, 1H, NH), 7.82 (d, J = 8.4 Hz, 2H, Ph), 7.70 (d, J = 8.4 Hz, 2H, Ph), 7.55 (d, J = 8.1 Hz, 2H, Ph), 7.33 (d, J = 8.1 Hz, 2H, Ph), 3.05-3.14 (m, 5H, CH + NCH₂), 2.60 (br, 4H, NCH₂), 2.35 (s, 3H, NCH₃), 2.09-2.12 (m, 1H, cyclopropane-CH₂), 1.82-1.89 (m, 1H, cyclopropane-CH₂), 1.18-1.62 (m, 10H, cyclohexane).

Compound **9b**, 1-amino-*N*-((1*S*,2*S*)-1-cyano-2-(4'-((4-methylpiperazin-1-yl)sulfonyl)-[1,1'-biphenyl]-4-yl)cyclopropyl)cyclohexane-1-carboxamide.

¹H NMR (CDCl₃, 300 MHz) δ : 7.98 (s, 1H, NH), 7.82 (d, *J* = 8.4 Hz, 2H, Ph), 7.70 (d, *J* = 8.4 Hz, 2H, Ph), 7.55 (d, *J* = 8.1 Hz, 2H, Ph), 7.33 (d, *J* = 8.1 Hz, 2H, Ph), 3.07 (br, 5H, CH + NCH₂), 2.53 (br, 4H, NCH₂), 2.30 (s, 3H, NCH₃), 2.06-2.13 (m, 1H, cyclopropane-CH₂), 1.82-1.87 (m, 1H, cyclopropane-CH₂), 1.18-1.59 (m, 10H, cyclohexane).

Compound **10a**, (*S*)-2-amino-*N*-((1*R*,2*R*)-1-cyano-2-(4'-((4-methylpiperazin-1-yl)sulfonyl)biphenyl-4-yl)cyclopropyl)-3-cyclopropylpropanamide.

(80 mg, 46%). ¹H NMR (DMSO-*d*₆, 300 MHz) δ : 7.91 (d, *J* = 8.1 Hz, 2H, Ph), 7.79 (d, *J* = 8.1 Hz, 2H, Ph), 7.67 (d, *J* = 8.1 Hz, 2H, Ph), 7.34 (d, *J* = 7.8 Hz, 2H, Ph), 3.11 (m, 1H, CH), 3.03 (m, 1H, CH), 2.89 (br, 4H, NCH₂), 2.37 (m, 4H, NCH₂), 2.13 (s, 3H, NCH₃), 2.05 (m, 2H, cyclopropane-CH₂), 1.19 (m, 2H, CH₂), 0.99-0.14 (m, 5H, cyclopropyl).

Compound **10b**, (*S*)-2-amino-*N*-((1*S*,2*S*)-1-cyano-2-(4'-((4-methylpiperazin-1-yl)sulfonyl)biphenyl-4-yl)cyclopropyl)-3-cyclopropylpropanamide.

(163 mg, 58%). ¹H NMR (DMSO-*d*₆, 300 MHz) δ : 7.92 (d, *J* = 8.4 Hz, 2H, Ph), 7.79 (d, *J* = 8.4 Hz, 2H, Ph), 7.67 (d, *J* = 8.1 Hz, 2H, Ph), 7.33 (d, *J* = 8.4 Hz, 2H, Ph), 3.13 (m, 1H, CH), 2.92 (br, 5H, CH + NCH₂), 2.36 (m, 4H, NCH₂), 2.13 (s, 3H, NCH₃), 1.98 (m, 2H, cyclopropane-CH₂), 1.27-0.04 (m, 7H, CH₂ + cyclopropyl).

Compound **11a**, (*S*)-2-amino-*N*-((1*R*,2*R*)-1-cyano-2-(4'-((4-methylpiperazin-1-yl)sulfonyl)-[1,1'-biphenyl]-4-yl)cyclopropyl)pent-4-ynamide.

(120 mg, 47%). ¹H NMR (CDCl₃, 300 MHz) δ : 7.83 (d, *J* = 8.4 Hz, 2H, Ph), 7.71 (d, *J* = 8.4 Hz, 2H, Ph), 7.57 (d, *J* = 7.5 Hz, 2H, Ph), 7.35 (d, *J* = 8.1 Hz, 2H, Ph), 3.38 (m, 1H, CH), 3.12 (br, 5H, CH + NCH₂), 2.53 (br, 4H, NCH₂), 2.30 (s, 3H, NCH₃), 2.14 (m, 3H, CH + cyclopropane-CH₂), 1.88 (m, 2H, CH₂).

Compound **11b**, (*S*)-2-amino-*N*-((1*S*,2*S*)-1-cyano-2-(4'-((4-methylpiperazin-1-yl)sulfonyl)-[1,1'-biphenyl]-4-yl)cyclopropyl)pent-4-ynamide.

(240 mg, 70%). ¹H NMR (CDCl₃, 300 MHz) δ 7.84 (d, *J* = 8.4 Hz, 2H, Ph), 7.73 (d, *J* = 8.4 Hz, 2H, Ph), 7.58 (d, *J* = 8.4 Hz, 2H, Ph), 7.34 (d, *J* = 8.1 Hz, 2H, Ph), 3.34 (m, 1H, CH), 3.06 (br, 5H, CH+NCH₂), 2.60 (br, 2H, CH₂), 2.53 (br, 4H, NCH₂), 2.30 (s, 3H, NCH₃), 2.17 (m, 1H, CH₂), 2.02 (m, 1H, CH), 1.86 (m, 1H, CH₂).

Compound **12a**, (*S*)-2-amino-*N*-((1*R*,2*R*)-1-cyano-2-(4'-((4-methylpiperazin-1-yl)sulfonyl)biphenyl-4-yl)cyclopropyl)-3-phenylpropanamide.

(90 mg, 13%). LC-MS: 544.2 (M+H)/calculated mass: 543.7. ¹H NMR (CDCl₃, 300 MHz) δ: 7.56 (d, *J* = 8.1 Hz, 2H, Ph), 7.68 (d, *J* = 8.1 Hz, 2H, Ph), 7.57 (d, *J* = 8.1 Hz, 2H, Ph), 7.49 (s, 1H, NH), 7.33 (d, *J* = 8.1 Hz, 2H, Ph), 7.25 (m, 3H, Ph), 7.08 (m, 2H, Ph), 3.48 (m, 1H, CH), 3.10 (m, 6H, CH+Bn+NCH₂), 2.52 (m, 4H, NCH₂), 2.29 (s, 3H, NH₃), 2.17 (m, 2H, Br+cyclopropane-CH₂), 1.87 (m, 1H, cyclopropane-CH₂).

Compound **12b**, (*S*)-2-amino-*N*-((1*S*,2*S*)-1-cyano-2-(4'-((4-methylpiperazin-1-yl)sulfonyl)biphenyl-4-yl)cyclopropyl)-3-phenylpropanamide.

(0.51 g, 67%). LC-MS: 544.2 (M+H)/calculated mass: 543.7. ¹H NMR (CDCl₃, 300 MHz) δ: 7.85 (d, *J* = 8.1 Hz, 2H, Ph), 7.72 (d, *J* = 8.1 Hz, 2H, Ph), 7.46 (m, 3H, Ph+NH), 7.31 (m, 3H, Ph), 7.11 (m, 4H, Ph), 3.51 (m, 1H, CH), 3.07 (m, 7H, CH+Bn+NCH₂), 2.54 (m, 4H, NCH₂), 2.30 (s, 3H, NCH₃), 2.14 (m, 1H, cyclopropane-CH₂), 1.74 (m, 1H, cyclopropane-CH₂).

Compound **13a**, (*S*)-2-amino-*N*-((1*R*,2*R*)-1-cyano-2-(4'-((4-methylpiperazin-1-yl)sulfonyl)biphenyl-4-yl)cyclopropyl)-3-(thiophen-2-yl)propanamide.

¹H NMR (CDCl₃, 300 MHz) δ: 7.82 (d, *J* = 8.4 Hz, 2H, Ph), 7.57 (d, *J* = 8.4 Hz, 2H, Ph), 7.48-7.53 (m, 3H, Ph+thiophene), 7.34 (d, *J* = 8.1 Hz, 2H, Ph), 7.14 (d, *J* = 5.1 Hz, 1H, thiophene), 6.89 (dd, *J* = 3.6 Hz, 5.1 Hz, 1H, thiophene), 6.72 (br, 1H, NH), 3.45-3.50 (m, 1H, CH), 3.06-3.18 (m, 6H, thiophene-CH₂+NCH₂), 2.55-2.64 (m, 1H, CH), 2.53 (m, 4H, NCH₂), 2.89 (s, 3H, NCH₃), 2.06-2.17 (m, 1H, cyclopropane-CH₂), 1.84-1.90 (m, 1H, cyclopropane-CH₂).

Compound **13b**, (S)-2-amino-N-((1*S*,2*S*)-1-cyano-2-(4'-(4-methylpiperazin-1-ylsulfonyl)biphenyl-4-yl)cyclopropyl)-3-(thiophen-2-yl)propanamide.

(180 mg, 35%). ¹H NMR (CDCl₃, 300 MHz) δ 7.83 (d, J = 8.4 Hz, 2H, Ph), 7.70 (d, J = 8.4 Hz, 2H, Ph), 7.48 (d, J = 8.4 Hz, 2H, Ph), 7.24 (m, 1H, thiophene), 7.12 (d, J = 8.4 Hz, 1H, thiophene), 7.02 (dd, J = 3.3 Hz, 5.1 Hz, 1H, thiophene), 6.84 (br, 1H, NH), 3.46-3.51 (m, 1H, CH), 3.27-3.35 (m, 1H, CH), 2.99-3.14 (m, 6H, thiophene-CH₂+NCH₂), 2.52-2.54 (m, 4H, NCH₂), 2.30 (s, 3H, NCH₃), 2.12-2.18 (m, 1H, cyclopropane-CH₂), 1.80 (t, J = 7.7 Hz, 1H, cyclopropane-CH₂).

Compound **14a**, (S)-2-amino-N-((1*R*,2*R*)-1-cyano-2-(4'-(4-methylpiperazin-1-ylsulfonyl)biphenyl-4-yl)cyclopropyl)-3-(furan-2-yl)propanamide.

(63 mg). LC-MS: 534.1/calculated mass: 533.1. ¹H NMR (CDCl₃, 300 MHz) δ: 7.80 (d, J = 8.4 Hz, 2H, Ph), 7.68 (d, J = 8.1 Hz, 2H, Ph), 7.55 (d+s, J = 8.1 Hz, 3H, Ph+Fura), 7.33 (d, J = 8.1 Hz, 2H, Ph), 6.23 (m, 1H, Fura), 5.98 (d, J = 3 Hz, 1H, Fura), 3.51 (m, 1H, COCH), 3.08 (m, 5H, NCH₂+PhCH+FuraCH₂), 2.51 (m, 4H, NCH₂), 2.38 (m, 1H, FuraCH₂), 2.28 (s, 3H, NCH₃), 2.13 (m, 1H, cyclopropane-CH₂), 1.86 (m, 1H, cyclopropane-CH₂).

Compound **14b**, (S)-2-amino-N-((1*S*,2*S*)-1-cyano-2-(4'-(4-methylpiperazin-1-ylsulfonyl)biphenyl-4-yl)cyclopropyl)-3-(furan-2-yl)propanamide.

(55 mg). LC-MS: 534.1/calculated mass: 533.1. ¹H NMR (CDCl₃, 300 MHz) δ 7.82 (d, J = 8.4 Hz, 2H, Ph), 7.70 (d, J = 8.4 Hz, 2H, Ph), 7.58 (br, 1H, CONH), 7.52 (d, J = 8.1 Hz, 2H, Ph), 7.34 (s, 1H, Fura), 7.20 (d, J = 8.1 Hz, 2H, Ph), 6.33 (s, 1H, Fura), 6.09 (d, J = 2.7 Hz, 1H, Fura), 3.48 (m, 1H, COCH), 3.07 (m, 7H, PhCHNCH₂+FuraCH₂), 2.53 (s, 4H, NCH₂), 2.29 (s, 3H, NCH₃), 2.18 (m, 1H, cyclopropane-CH₂), 1.77 (m, 1H, cyclopropane-CH₂).

NMR analysis on synthesized compounds were performed by PepTech.

2.2. IC₅₀ determination

Human recombinant CatC was produced in baculovirus-infected cells²³ (Unizyme

Laboratories A/S, Hørsholm, Denmark) and activated at 4-6 °C with 5 mM cysteamine for 5 minutes and stored at -20 °C in a buffer containing 2.5 mM Na-phosphate, 150 mM NaCl, 2 mM cysteamine, 50% glycerol, pH 7.0 at a concentration of 1-2 mg/mL (5-10 μ M).

The IC₅₀ values of the nitrile inhibitors (compounds **1-14**) for human CatC were determined using Gly-Phe-pNA (*para*-nitroanilide) (Sigma, Denmark) as a substrate in 20 mM citric acid, 150 mM NaCl, 2 mM EDTA pH 4.5. The substrate was solubilized in DMF to give a 0.2-0.5 M stock solution, which was then further diluted with stirring in assay buffer to a final concentration of 1 mM. The concentration of the substrate used in the assay was 0.75 mM which is about 5 times below the K_m identified in this study (K_m= 3.9 mM).

A stock solution of human CatC was diluted 500-1000 times in assay buffer to a concentration of 10 nM. The assay was performed in 96-well plates. Diluted enzyme (25 μ L) was added to the well, followed by 25 μ L of test substance in varying concentrations, and the solution was mixed. The plate was incubated at 37 °C for 5 min, followed by addition of 150 μ L of 1 mM substrate prewarmed to 37 °C (corresponding to a substrate concentration of 750 μ M and a CatC concentration of 1.25 nM in the assay). The absorption was measured at 405 nm at 37 °C for every 90 sec for 12 min or every 20 sec for 4 min. Each measurement was made in duplicate. IC₅₀ was determined using a 4-parameter logistic equation in a non-linear curve fitting routine.

2.3. Downstream effect of CatC inhibition on NE/PR3 and CatG activation

The pro-monocytic cell line U937 was purchased from Health Protection Agency Culture Collection (HPACC) (Porton Down, Salisbury, UK) and maintained in suspension in RPMI 1640 containing 10% fetal bovine serum, 10 mM Hepes, 1 mM sodium pyruvate and 100 units/mL of each of penicillin and streptomycin in a humidified atmosphere of 5% CO₂ at 37 °C.

U937 cells were seeded in 12-well plates at 0.2 to 0.4×10^6 cells/mL in volumes of 1.5 mL per well in the presence of no or increasing concentrations of CatC inhibitor (compounds **2-14**). Twelve points in duplicate in the range of 0.02 nM to 50 μ M inhibitor were tested. After 24 or 48 h cells were harvested, washed twice with PBS and lysed in 20 mM Tris-HCl, pH 7.5 , 100 mM NaCl, 0.2% Triton X- 100 . Debris was removed by centrifugation and supernatants were retained. The extracts were mixed with assay buffer (50 mM Tris, 0.1% Triton X- 100 , 0.5 M NaCl, pH 8.0) supplemented with NE/PR3 substrate MeOSuc-AAPV-pNA (Bachem, Germany) to a final concentration of 0.9 mM, The activity of NE/PR3 was determined by measuring the enzymatic release of chromogenic *p*-nitroaniline (pNA) from the substrate which leads to an increase in absorbance at 405 nm. Assays were carried out in 96 -well plates in a final volume of 200 μ L at 37 °C, and absorbance was measured 8 times during 35 min using a plate reader. IC_{50} was determined using a 4-parameter logistic equation in a non-linear curve fitting routine.

2.4. Crystallization and structure determination of dipeptidyl cyclopropyl nitrile inhibitors in complex with human CatC

CatC preparation: CatC was diluted $1:1$ in dialysis buffer and dialyzed (Spectra/Por RC membrane molecular weight cutoff $6-8$ kDa) three times overnight against the following dialysis buffer: 2 mM cysteamine, 50 mM NaCl and 2.5 mM $NaPO_4$ pH 7.0 . The next day the protein solution was supplemented with 1.5 mM dithiothreitol (DTT) and concentrated to 11 mg/mL in an Amicon concentrator with molecular weight cutoff 10 kDa. The protein was used immediately for crystallization trials.

Crystallization: Compound **5a** was diluted in DMSO to obtain a 50 mM solution. 49 μ L of CatC solution were mixed with 1 μ L of compound **5a**. CatC was incubated with compound **5a** on ice for 1.5 h before crystallization. The crystal was grown from the JCSG-plus screen (Molecular Dimensions), condition B9, at 18 °C from a $100 + 100$ nL hanging

drop containing 20% (w/v) PEG 6 000, 0.1 M sodium citrate, pH 5.0. An intergrown crystal appeared within a few days. Cryoprotectant solution with the following composition was added to the drop: 16% (w/v) PEG 3.000, 0.08 M sodium citrate pH 5.0, 2.5 mM DTT, 20% v/v glycerol. The crystal was cut in pieces with crystal manipulation tools. The largest fragment containing a single crystal measuring approximately 0.1 x 0.1 x 0.1 mm was cryo-cooled in the liquid N₂ stream at the beamline.

Compound **9a** was diluted in DMSO to obtain a 100 mM solution. 49.5 µL of CatC solution were mixed with 0.5 µL of compound **9a**. The protease was incubated with compound **9a** on ice for 2 h before crystallization set-ups. The crystal was grown from a 2 + 2 µL sitting drop in a microbridge (Molecular Dimensions) placed in a NeXtal plate (Qiagen) at 18 °C containing: 20% (w/v) PEG 3 000, 0.2 M ammonium citrate dibasic. DTT was added to the reservoir to 2 mM immediately after drop setup. Crystals appeared overnight. Cryoprotectant solution with the following composition was used: 20% (w/v) PEG 3.000, 0.2 M ammonium citrate dibasic, 2.5 mM DTT, 20% (v/v) glycerol, 0.5 mM of compound **9a**. A crystal measuring 0.25 x 0.25 x 0.1 mm was flash-cooled in liquid N₂.

Compound **13a** was crystallized similarly to compound **9a**, with the following differences: the reservoir solution was 20% (w/v) PEG 3 000, 0.1 M sodium citrate pH 5.6 and the cryoprotectant solution was: 20% (w/v) PEG 3 000, 0.1 M sodium citrate pH 5.6, 2.5 mM DTT, 20% (v/v) glycerol, 0.5 mM of compound **13a**. The crystal used measured 0.3 x 0.3 x 0.1 mm.

Data collection: Data for compound **5a** were collected at 100 K at station I911-2 of the MAX-lab synchrotron, Lund, Sweden ($\lambda = 1.03796$ Å), equipped with a 165mm marCCD detector. The data were collected in a single pass, processed using XDS and reduced using the CCP4 suite. Data for compound **9a** and compound **13a** were collected at 100 K on a Proteum X8 laboratory X-ray system from Bruker consisting of a Microstar microfocus X-ray source

($\lambda = 1.5418 \text{ \AA}$), Montel optics, kappa goniometer, Pt135 CCD detector and Cryoflex cryo system. Complete data were collected to 2.15 \AA at the radial edge of the square detector. Diffraction was obtained into the corners of the detector, to 2.0 \AA resolution, albeit with lower completeness. Data were processed using the Proteum2 software from Bruker and reduced using the CCP4 suite.

Structure determination and refinement: The structures of CatC in complex with compound **5a**, compound **9a** and compound **13a** were solved by difference Fourier methods using another in-house CatC complex. The difference map showed clear electron density for all ligands. Geometric restraints files for the ligands and their covalent bonds to Cys234 were generated using energy-minimized coordinates from Schrödinger Suite 2009 (Schrödinger Inc.) and the JLigand⁴¹ tool in the CCP4 program suite.⁴² The model was refined using Refmac5⁴³ combined with manual rebuilding using Coot.⁴⁴ Riding hydrogen atoms were added during refinement. A separate TLS group⁴⁵ was used for each protein chain. Data collection and refinement statistics for inhibitor/CatC complexes are shown in Table 2.

The structure of compound **8a** was not determined by X-ray crystallography but was computationally modelled. The necessary information about interactions of each end of the compound **8a** was given by the other structures in which these moieties were present, so it was considered unnecessary to determine the structure of compound **8a**. The ethyl moiety of compound **8a** is found in the crystal structure of compound **5a** and the outer piperazine-sulfonyl moiety is in the crystal structures of compound **9a** and compound **13a**.

2.5. Human and mouse plasma stability analysis of IcatC_{XPZ-01}

Studies (service provided by Absorption Systems (Exton, PA, USA)) were carried out in mixed-gender plasma collected on sodium heparin. Plasma was adjusted to pH 7.4 prior to initiating the experiments. DMSO stocks were first prepared for the test articles. Aliquots of

the DMSO solutions were dosed into 1 mL of plasma, which had been pre-warmed to 37 °C, at a final **IcatC_{XPZ-01}** concentration of 1 µM. The vials were kept in a benchtop Thermomixer® for the duration of the experiment. Aliquots (100 µL) were taken at each time point (0, 15, 30, 60, and 120 min) and added to 96-well plates which had been pre-filled with 300 µL of acetonitrile (ACN). Samples were stored at 4 °C until the end of the experiment. After the final time point was sampled, the plate was mixed and then centrifuged at 3,000 rpm for 10 min. Aliquots of the supernatant were removed, diluted 1:1 into distilled water, and analyzed by LC-MS/MS. The peak area response ratio (PARR) to internal standard metoprolol was compared to the PARR at time 0 to determine the percent remaining at each time point. Half-lives were calculated using GraphPad software, fitting to a single-phase exponential decay equation.

2.6. Microsomal half-life determination of **IcatC_{XPZ-01}**

Microsomal half-life determination was performed by Arbsorption Systems (Exton, PA, USA). **IcatC_{XPZ-01}**, compound **7a** and compound **12a** were dissolved in 100% DMSO at a concentration of 10 mM. The reaction mixture, consisted of mouse or human liver microsomes (1.0 mg/mL), 1 mM NADPH, 100 mM KH₂PO₄, 10 mM MgCl₂, pH 7.4, and the test compound at a concentration of 5 µM.

An aliquot of the reaction mixture (without cofactors) was incubated in a shaking water bath at 37 °C for 3 min. Another aliquot of the reaction mixture was prepared as the negative control. The test compound was added into both the reaction mixture and the negative control at a final concentration of 5 µM.

The reaction was initiated by the addition of NADPH to 1 mM (not into the negative controls) and then incubated in a shaking water bath at 37 °C. Aliquots (100 µL) were withdrawn at 0, 10, 20, 30, and 60 min or at 0, 15, 30 and 60 min and combined with 900 µL

of ice-cold 50/50 acetonitrile/dH₂O to terminate the reaction. A control (testosterone) was run simultaneously with the test compound in a separate reaction. LC/MS/MS is used to determine the peak area response ratio (peak area corresponding to the test compound or control divided by that of metoprolol used as the analytical internal standard). The natural log of the percent remaining was plotted versus time. A linear fit was used to determine the rate constant. The fit was truncated if the percent remaining of test compound was less than 10%. The elimination half-lives associated with the disappearance of the test and control compounds were determined to compare their relative metabolic stability.

2.7. Test for inhibition of CYP2C9, CYP2D6 and CYP3A4 enzymes (IC₅₀ Determination)

Testing for CYP inhibition potential was a service provided by Arbsorption Systems (Exton, PA, USA). The test compounds, at eight concentration levels (0, 0.137, 0.412, 1.23, 3.70, 11.1, 33.3 and 100 μ M), were incubated with pooled human liver microsomes (0.25 mg protein/mL) at 37 °C in the presence of phosphate buffer (100 mM, pH 7.4), MgCl₂ (5 mM), NADPH (1 mM), and CYP-specific probe substrate at approximately K_m (6 μ M diclofenac, 7 μ M bufuralol and 75 μ M testosterone for CYP2C9, CYP2D6, and CYP3A4, respectively). After a period of incubation, samples were treated by the addition of protein precipitation solvent and centrifuged. CYP enzyme activities were measured by determining the formation of the CYP probe metabolites by LC-MS/MS, and the IC₅₀ (the concentration of an inhibitor causing 50% inhibition) was estimated using GraphPad Prism® software by fitting the experimental data (percent of control activity remaining at each concentration of test compound) to a sigmoidal model and non-linear regression analysis.

The CYP enzyme activities in the human liver microsomes were verified in parallel by determining the inhibition of positive inhibitors on the CYP enzyme activities (sulfaphenazole, quinidine and ketoconazole for CYP2C9, CYP2D6, and CYP3A4, respectively). All CYP

enzymes showed expected inhibitions by positive inhibitors, indicating that the human liver microsomes used in this study were metabolically active and responsive.

2.8. Test for hERG Channel Inhibition (IC_{50} Determination)

The experiments were performed (as a service provided by Cypotex Discovery Ltd. (Cheshire, UK)) on an IonWorksTM HT instrument (Molecular Devices Corporation), which automatically performs electrophysiology measurements in 48 single cells simultaneously in a specialized 384-well plate (PatchPlateTM). All cell suspensions, buffers and test compound solutions were at RT during the experiment.

The cells used were Chinese hamster ovary (CHO) cells stably transfected with hERG (cell line obtained from Cytomyx, UK). A single cell suspension was prepared in extracellular solution (Dulbecco's phosphate buffered saline with calcium and magnesium pH 7-7.2) and aliquots added automatically to each well of a PatchPlateTM. The cells were then positioned over a small hole at the bottom of each well by applying a vacuum beneath the plate to form an electrical seal. The vacuum was applied through a single compartment common to all wells which was filled with intracellular solution (buffered to pH 7.2 with HEPES). The resistance of each seal was measured *via* a common ground electrode in the intracellular compartment and individual electrodes placed into each of the upper wells.

Electrical access to the cell was then achieved by circulating a perforating agent, amphotericin, underneath the PatchPlateTM and then measuring the pre-compound hERG current. An electrode was positioned in the extracellular compartment and a holding potential of 80 mV applied for 15 sec. The hERG channels were then activated by applying a depolarising step to +40 mV for 5 sec and then clamped at 50 mV for 4 sec to elicit the hERG tail current, before returning to 80 mV for 0.3 sec.

IcatC_{XPZ-01} was then added automatically to the upper wells of the PatchPlateTM from a 96-well microtitre plate containing a range of concentrations of each compound. Solutions

were prepared by diluting 10 mM DMSO solutions of the test compound into extracellular buffer such that the final concentrations tested were 0.008, 0.04, 0.2, 1, 5 and 25 μ M (final DMSO concentration 0.25%). **IcatC_{XPZ-01}** was left in contact with the cells for 300 sec before recording currents using the same voltage step protocol as in the pre-compound scan. Quinidine, an established hERG inhibitor, was included as a positive control and buffer containing 0.25% DMSO was included as a negative control. The results for all compounds on the plate were rejected and the experiment repeated if the IC₅₀ value for quinidine or the negative control results were outside quality control limits.

Each concentration was tested in 4 replicate wells on the PatchPlate™. However, only cells with a seal resistance greater than 50 MOhm and a pre-compound current of at least 0.1 nA were used to evaluate hERG blockade.

Post compound currents were then expressed as a percentage of pre-compound currents and plotted against concentration for each compound. Where concentration dependent inhibition was observed, the data were fitted to the following equation and an IC₅₀ value calculated:

$$y = \frac{y_{\max} - y_{\min}}{1 + (x/x_{50})^s} + y_{\min}$$

Where y = (post compound current/pre compound current) x 100, x = concentration,

x₅₀ = concentration required to inhibit current by 50% (IC₅₀) and s = slope of the graph

2.9. Animal experiments, observations and examinations

The evaluation of **IcatC_{XPZ-01}** in the collagen antibody induced mouse model of rheumatoid arthritis was performed by Inflammations Discovery Services at MD Biosciences (Glasgow, UK). 46 young adult BALB/c male mice (6-8 weeks at study initiation) in good health were acclimatized to laboratory conditions. During 10-day acclimation period and following dosing, animals were housed within a limited access rodent facility and kept in groups of 5. Mice were housed in sterilized individually ventilated polysulfone cages with

sterile wood shavings as bedding materials. Animals were provided *ad libitum* a commercial rodent diet and free access to drinking water, supplied to each cage via sterilized polyethylene bottles with stainless steel sipper tubes. All food and water were sterilized. Automatically controlled environmental conditions were set to maintain temperature at 20-24 °C with relative humidity (RH) of 30-70%, a 12:12 h light:dark cycle and 90 air changes/h in individually ventilated cages. Temperature, RH and light cycle were monitored daily by the control computer. Animals were given a unique animal identification number. This number also appeared on a cage card, visible on the front of each cage. The cage card also contained the study number. Animals were randomly assigned to experimental treatment groups. Treatment groups were distributed across experimental cages. At the end of the study surviving animals were euthanized by CO₂ asphyxiation followed by cervical dislocation. This study was performed according to the UK Home Office regulations for use of animals in scientific procedures - Animals (Scientific Procedures) Act 1986.

Arthritis induction: As shown in the schematic depiction (**Figure 7**), all animals were subjected on day 0 of the study (*study commencement*) to a tail vein injection of ArthritoMAbTM monoclonal antibody (mAb) cocktail (2 mg/mouse). mAb stock solution (10 mg/mL), supplied by MD Biosciences, Division of Morwell Diagnostics GmbH, was used as provided. Three days post the single mAb administration, all animals were subjected to LPS (MD Biosciences) administration by a single intraperitoneal injection (100 µg/mouse). LPS was diluted with PBS to achieve the appropriate concentration. Thorough vortexing was required just prior to its injection.

Treatment administration: **IcatC_{XPZ-01}** (1.2 mg/kg or 4.8 mg/kg at 10 mL/kg) and vehicle control (10 mL/kg) were administered twice daily with a 12 h separation between doses, from day -14 to day 11 by subcutaneous injection. To ensure that neutrophils in circulation have been exposed to **IcatC_{XPZ-01}** at the promyelocyte stage and beyond where

elastase-like proteases are formed and stored, animals were treated with IcatC_{XPZ-01} for 14 days before arthritis induction. The vehicle 2-hydroxypropyl- β -cyclodextrin (HP β CD) (Sigma) was dissolved in 50 mM citrate buffer (pH 5.0) (Sigma-Aldrich, Denmark) to make a 15% HP β CD solution for injection. The positive control (Enbrel) was administered once daily from day 0 to day 11 by intraperitoneal injection (6.25 mg/kg at 10 mL/kg). A stock solution of Enbrel (Wyeth Pharmaceuticals) was formulated according to the manufacturer's instructions and diluted in PBS to the required concentration shortly before each daily administration.

On day -15 all the animals were assigned to treatment groups 1, 2, 3 and 4. The dose administered was calculated based on the assumption that the animals weighed, on average, 20 g. A fixed volume of 200 μ L was administered to each mouse. No analgesia was used during the course of the study.

Bone marrow sample collection: Four mice from the vehicle (GROUP 1), IcatC_{XPZ-01} 1.2 mg/kg (GROUP 2) and IcatC_{XPZ-01} 4.8 mg/kg (GROUP 3) treated groups were terminated at 1 h (day 11) and 12 h (day 12) post the last dose. Four mice from the IcatC_{XPZ-01} 1.2 mg/kg and IcatC_{XPZ-01} 4.8 mg/kg treated groups and five mice from the vehicle treated group were terminated at 24 h (day 12) after the last dose was administered. No samples were obtained from mice treated with the positive control (Enbrel). At each time point, both rear paws from all animals were removed and used to extract bone marrow. The bone marrow was made into a single cell suspension, cell number was determined and the cells were then pelleted and snap frozen. The pellets were dried using a pipette to ensure a minimal amount of liquid remained. The cells were stored at -80 °C.

Bone marrow extract preparation: Pellets of bone marrow cells were resuspended in 400 μ L buffer C (50 mM Tris, 0.5 M NaCl, pH 7.5 supplemented with Benzonase (Merck, Cat.no.: 101654) to 250 u/mL and supplemented with Triton X-100 to a concentration of 0.2%). Suspensions became clear within a few minutes and were then diluted with 300 μ L

buffer B (50 mM Tris, 0.5 M NaCl, pH 7.5 supplemented with Benzonase). Extracts were mixed and cell debris was removed by centrifugation 20.000 x g, 4 °C, 2 min. Concentrations of protein in supernatants were determined using the Bradford method. All samples were measured in duplicate and in two different dilutions.

Proteolytic activity measurement: 50 mM stock solution of NE/PR3 substrate MeOSuc-Ala-Ala-Pro-Val-pNA (Bachem Cat. No.: L-1335) prepared in DMSO was stored at RT and used for assays within 10 days after preparation. 1.09 mM working solution was prepared from the 50 mM stock solution by dilution in 50 mM Tris, 0.5 M NaCl, pH 7.5 and pre-warmed to 37 °C just prior to assay. 50 mM stock solution of CatG substrate Suc-Ala-Ala-Pro-Phe-pNA (Bachem Cat. No.: L-1400) prepared in DMSO was stored at RT and used for assays within 10 days after preparation. 2.5 mM working solution was prepared from the 50 mM stock solution by dilution in 50 mM Tris, 0.5 M NaCl, pH 7.5 and pre-warmed to 37 °C just prior to assay.

160 µL of NE/PR3 or CatG substrate (working solution) were mixed with 40 µL of bone marrow supernatants (previously diluted 10-20 times in 50 mM Tris, 0.5 M NaCl, pH 7.5) in 96-well plates and assayed in a Microplate Reader BioTek Elx808) NE/PR3 and CatG substrates were used, respectively, at 0.875 and 2 mM final in assay. Absorbance (405 nm) were measured every 2 min for 30 min at 37 °C.

Body weight measurement: Determination of individual body weights of animals were made three times weekly from study day -14, shortly before arthritis induction on day 0 (*study commencement*) and subsequently on study days 3-8, 10, 11 and 12.

Clinical signs examination: Careful clinical examinations were carried out three times weekly from study day -14, shortly before arthritis induction on day 0 and subsequently on study days 3-8, 10, 11 and 12. Observations included changes in skin, fur, eyes, mucous membranes, occurrence of secretions and excretions (e.g. diarrhoea) and autonomic activity

(e.g. lacrimation, salivation, piloerection, pupil size, unusual respiratory pattern). Changes in gait, posture and response to handling, as well as the presence of bizarre behaviour, tremors, convulsions, sleep and coma were also noted.

Arthritis reactions measurements: **All paws (front and rear) of each animal were examined for signs of arthritogenic responses prior to Test Item or control item administration on study day 0 (study commencement) and subsequently on study days 3-8, 10, 11 and 12.** Arthritis reactions were scored and recorded according to a 0-4 scale in ascending order of severity as shown below:

Arthritis Score	Grade
No reaction, normal	0
Mild, but definite redness and swelling of the ankle/wrist or apparent redness and swelling limited to individual digits, regardless of the number of affected digits	1
Moderate to severe redness and swelling of the ankle/wrist	2
Redness and swelling of the entire paw including digits	3
Maximally inflamed limb with involvement of multiple joints	4

The thickness of both hind paws (left & right, just above the foot pad and below the calcaneum) of each animal was measured in mm on study day 0 (study commencement) and subsequently on study days 3-8, 10, 11 and 12. Paw thickness was measured using a dial caliper (Kroeplin, Munich, Germany).

Evaluation was primarily based on the mean values for arthritis scoring and paw thickness measurements. Where appropriate, analysis of the data by ANOVA with Tukey post hoc analysis was applied to determine significance of treatment effects.

3. Results

3.1. Design and synthesis of novel potent cell-permeable dipeptidyl cyclopropyl nitrile inhibitors of human CatC

The dipeptidyl nitrile compound **1** with a (*S*)-2-amino butyric acid at P2 position and a biphenyl at P1 position has been previously identified as a potent and selective dipeptidyl nitrile inhibitor of human CatC (half maximal inhibitory concentration, $IC_{50} = 13 \pm 3 \text{ nM}^{31}$) and was used here as a template for the development of new nitrile inhibitors of CatC. The addition of *p*-fluoro or *p*-trifluoromethyl on the biphenyl moiety of compound **1** yielding compound **2** and compound **3** resulted in most potent CatC inhibitors with IC_{50} values of 5.5 nM and 1.7 nM, respectively (**Table 3**). However, all three inhibitors displayed relatively poor reactivity in cellular assays using U937 cells due to the rapid hydrolysis of their amide bond in the cell assay medium and in plasma (*not shown*).

We inserted a 1,1-cyclopropyl amino nitrile moiety at P1 in compound **2** and compound **3** to tentatively prevent hydrolysis and increase the *ex-vivo* and *in vivo* stability of the inhibitor. The resulting compounds were fractionated into S,R,R (compounds **4a** and **5a**) and S,S,S (compounds **4b** and **5b**) isomers. S,R,R isomers were clearly more efficient than S,S,S isomers at inhibiting CatC ($IC_{50} = 18 \text{ nM}$ for compound **4a** vs 1060 nM for compound **4b**; $IC_{50} = 15 \text{ nM}$ for compound **5a** vs 1390 nM for compound **5b**). Further, compound **4a** and compound **5a** resisted hydrolysis in the cell assay medium and in plasma though IC_{50} values increased significantly using a U937 cell based inhibition assay (**Table 3**). We then solved the crystal structure of the human CatC-compound **5a** complex to direct the synthesis of additional dipeptidyl cyclopropyl nitrile inhibitors from compound **5a** with improved cell permeability and cellular potency. Compound **5a** is located in the active site area, with the P1 side chain 4'-(trifluoromethyl)biphenyl pointing toward the solvent and the trifluoromethyl group facing proline 3 (measured distance $\sim 3\text{\AA}$) in the exclusion domain whereas the nitrile group clearly made a covalent bond with Cys234 of the CatC active site (**Figure 4A**). The amino group of the inhibitor makes two potential H-bonds to the side chain of Asp1. Its peptide carbonyl group makes an H-bond to the main chain amine group of Gly277 and the

peptide amine makes one to the main chain carbonyl of Asn380. To improve the cell permeability and cellular potency of the inhibitor we replaced the *p*-trifluoromethyl group on the biphenyl moiety in compound **5** by 4-methylpiperazin (compound **6**), (4-methylpiperazin-1-yl)-[1,2,4]triazolo[1,5-*a*]pyridin-6-yl)phenyl (compound **7**) and 4'-(4-methylpiperazin-1-ylsulfonyl) (compound **8**). These substitutions significantly improved the cellular potency of all these new compounds (compound **6a**, $IC_{50} = 74$ nM; compound **7a**, $IC_{50} = 17$ nM; compound **8a**, $IC_{50} = 6$ nM) as compared to compound **5a** (Table 3). However, the insertion of a terminal 4-methylpiperazin group significantly impaired the potency of compound **6a** for purified CatC ($IC_{50} = 661$ nM). A rotameric analysis performed by attaching the 4-methylpiperazin to the compound **5a** on the solved crystal structure showed that the 4-methylpiperazin in compound **6a** has multiple clashes with Pro3, which may result in the loss of the crucial hydrogen bond between Asp1 and the N-terminal amino group of the inhibitor. The potency of compound **7a** ($IC_{50} = 52$ nM) and compound **8a** ($IC_{50} = 15$ nM) for purified CatC was significantly better than that of compound **6a** and this was consistent with the orientation of 4-methylpiperazin-1-yl)-[1,2,4]triazolo[1,5-*a*]pyridin-6-yl)phenyl and 4'-(4-methylpiperazin-1-ylsulfonyl) within computationally-modeled complexes with CatC (Figure 5). In this case we did not observe any clash of the inhibitor with the protein and we retained compound **8a** as the most reliable inhibitor.

Next step was to tentatively improve the potency of compound **8a** by exchanging the (*S*)-2-amino butyric acid at P2 position in compounds **9a-14a** (Table 3). The substitutions significantly improved IC_{50} values of compound **13a** and compound **14a** but impaired the IC_{50} of compounds **9a-10a**. CatC complexes with compound **9a** or with compound **13a** were crystallized and the overall binding was compared to that with compound **5a**. The backbones of three inhibitors in crystal structures were identical and differed only at their extremities, one on the protein surface and the other deep in the binding pocket (Figure 4). The

compounds make the same four hydrogen bonds with the protein backbone and amino-acid side-chains. Moreover, the NH₂ groups of the inhibitors are similarly oriented, all donating hydrogens to the side chain of Asp1 in the S2 pocket (**Figure 4**). The compound **13a** ((*S*)-2-thienylmethyl)) and compound **14a** ((*S*)-2-furanylmethyl)) with higher potency displayed an only moderate metabolic stability (mouse microsomal half-life: compound **13a**, $t_{1/2}$ = 2.4 min; compound **14a**, $t_{1/2}$ = 2.4 min, **Table 4**) as compared to compound **8a** (mouse microsomal half-life: $t_{1/2}$ = 11 min; human microsomal half-life: $t_{1/2}$ = 43 min, **Table 4** and **Table 5**). Compound **8a** also turned out to be very stable in human and mice plasma with a half-life of ~120 min. Profiling the human ether-a-go-go-related gene (hERG) potassium channel showed safety with an IC₅₀ >25 μ M. Moreover, compound **8a** did not show significant inhibition of the cytochromes P450 (CYP450) enzymes. From the profiling data generated here (**Table 4** and **Table 5**), it was clear that compound **8a**, now called **IcatC_{XPZ-01}**, was the most appropriate for *in vivo* assays.

3.2. Pharmacokinetic profile of IcatC_{XPZ-01}

We first checked that **IcatC_{XPZ-01}** retained similar inhibitory properties towards rodent and human CatC. Then the pharmacokinetics of **IcatC_{XPZ-01}** were evaluated after subcutaneous dosing in male Balb/c mice. Plasma and bone marrow samples were collected up to 48 h post dose and levels of **IcatC_{XPZ-01}** were determined by LC-MS/MS (**Figure 6**). Concentration *versus* time data was analyzed using a non-compartment pharmacokinetic model. Following a single subcutaneous dose of 4.8 mg/kg in group 1 mice, maximum plasma concentrations (758 ± 82 ng/mL) were observed at 15 min post dosing and the bioavailability was 78%. With a second 4.8 mg/kg dose at 12 h (group 2), steady state levels were increased because of the higher input (**Figure 6A**, **Table 6**). Due to the very low sample size, triplicate bone marrow samples from mice within each time point were pooled together for analysis.

IcatC_{XPZ-01} was detectable in all bone marrow samples till 48 h post dosing in both groups (**Figure 6B**).

3.3. Rationale for *in vivo* drug testing doses

A substantial inhibition of CatC is required for *in vivo* blockage of proNSPs processing³⁷. Our presumption was that in order to achieve a significant reduction of the proteases and a pharmacological effect of **IcatC_{XPZ-01}**, the inhibitor concentration in the target tissue (bone marrow) should constantly be equal to or exceed the concentration that inhibits >95% of CatC. From U937 inhibition curves it was estimated that IC₉₉ for **IcatC_{XPZ-01}** is approximately 700 nM in the cell-based assay. The pharmacokinetic study (**Figure 6B**) indicated that 4.8 mg/kg dosed twice daily constantly would keep the inhibitor concentration in bone marrow above 1400 nM. In order to obtain a high fractional inhibition of CatC, and to ideally demonstrate a dose dependent effect of **IcatC_{XPZ-01}**, it was chosen to treat twice daily with 1.2 mg/kg and 4.8 mg/kg corresponding to 2.5 and 10 µmol/kg.

3.4. Evaluation of **IcatC_{XPZ-01}** in a mouse model of rheumatoid arthritis

The efficacy of **IcatC_{XPZ-01}** was evaluated in a mouse model of collagen antibody-induced arthritis (CAIA). Mice were treated subcutaneously twice daily with vehicle (negative control GROUP 1) or **IcatC_{XPZ-01}** at 1.2 mg/kg (GROUP 2) or 4.8 mg/kg (GROUP 3) (**Figure 7**). Enbrel, a biopharmaceutical used to treat patients with autoimmune diseases by inhibiting TNF-α activity, was administrated by intraperitoneal injection as positive control (GROUP 4). One Enbrel treated mouse was terminated on study day -1 due to severe, self-inflicted bite marks on the tail. No other mortality occurred throughout the duration of the study.

Bone marrow was extracted from four mice treated with the vehicle (GROUP 1), **IcatC_{XPZ-01}** 1.2 mg/kg (GROUP 2) or **IcatC_{XPZ-01}** 4.8 mg/kg (GROUP 3) at approximately 1 h, 12 h and 24 h post-last dose administered at day 11. There was no reduction in cell numbers in bone marrow cell samples from **IcatC_{XPZ-01}** treated mice compared to mice treated with vehicle. In bone marrow cellular lysates from the mice treated with **IcatC_{XPZ-01}**, we observed a dose dependent significant reduction of both NE/PR3 and CatG activities compared to the vehicle group (**Figure 8**).

Following arthritis induction, increasing arthritis reactions were found in the vehicle group from day 4 (mean total arthritis scores and mean rear paw arthritis scores) or from day 5 (mean rear paw thickness). After peaking at day 8 or 10, respectively, arthritis scores and paw thickness slowly decreased. As shown in Figure 9, slightly fluctuating arthritis reactions were also found in the Enbrel and IcatC treated groups but arthritis scores and paw thickness were considerably lower throughout the study period. Treatment with **IcatC_{XPZ-01}** at 1.2 mg/kg and 4.8 mg/kg significantly reduced total arthritis scores on days 6 to 11, and days 6 and 8 to 11, respectively, when compared to treatment with the vehicle. Likewise, treatment with Enbrel reduced total arthritis scores when compared to treatment with the vehicle, but significance was only found on day 10 (**Figure 9A**). Rear paw arthritis scores and rear paw thickness were significantly reduced on the majority of the study days 6 to 12 in both **IcatC** treatment groups and in the Enbrel treatment group (**Figure 9B,C**). In summary, the results showed that subcutaneous treatment with **IcatC_{XPZ-01}** at 1.2 mg/kg and 4.8 mg/kg exhibited statistically significant anti-arthritic activity with sustained reductions in arthritis scores and paw thickness comparable or even better than that found for Enbrel. No statistically significant difference was found at any study day between the two doses of **IcatC_{XPZ-01}**.

The results also showed that the 26-days treatment with **IcatC_{XPZ-01}** was well tolerated. No clinical signs unrelated to arthritis was observed from day -14 to day -2, and clinical signs

related to lipopolysaccharide (LPS) administration (day 3) were as expected observed on days 4 to 8. Mean body weight increased in all treatment groups from day -14 to day 3. Following LPS administration on day 3, weight decreased until day 5 and then increased again until day 12. No significant differences in body weight were observed between any of the treatment groups and the vehicle treated group throughout the duration of the study.

4. Discussion

CatC is involved in the processing and maturation of immune cell associated serine protease zymogens.² It plays a major role in the activation of pro-inflammatory NE-like proteases.^{2, 10} Inhibition of the the bone marrow CatC has been explored as a potential therapeutic option to treat chronic inflammatory or auto-immune diseases dominated by neutrophils.^{2, 10, 21, 40} The purpose of the work presented here was to develop a CatC inhibitor with potency and pharmaceutical properties suitable for clinical development and to evaluate its efficacy in a disease model *in vivo*.

A widely used warhead in inhibitors targeting cysteine proteases is the nitrile group that binds covalently but reversibly to the nucleophilic cysteine residue of the active site.⁴⁶ The first dipeptide-derived nitrile inhibitors of CatC were described a decade ago.³¹ The most potent inhibitor of CatC contained an aminobutyramide group in P2 and a lipophilic 4-biphenylalanine in P1. More recently, Guay et al. developed a series of inhibitors with a 2-thienylalanine residue in P2, that inhibit CatC with subnanomolar IC₅₀ values.³³ Inopportunely, all reported dipeptide-derived nitrile inhibitors of CatC were rapidly degraded in circulation. Nevertheless the same authors established that the steric hindrance in the vicinity of the amide bond achieved by the insertion of a 1,1-cyclopropyl amino nitrile moiety makes these derivatives resistant to hydrolytic cleavage.³³ A major drawback of the most potent and

resistant inhibitors of this series, however, still remained: they all retained a poor half-life *in vivo*.

Our starting point for the development of further compounds with improved properties was the dipeptide-derived nitrile inhibitor reported in 2006 by Bondebjerg et al.³¹ Insertion of a 1,1-cyclopropyl amino nitrile moiety at P1 in *p*-chloro, *p*-phenyl and *p*-methylpiperazine-1-sulfonyl substituted derivatives generated potent CatC inhibitors with IC₅₀ values around 15 nM that were also highly stable in whole blood. The cyclopropyl-derived dipeptidyl compounds are featured by the presence of three chiral carbon atoms in the backbone. The configuration of these chiral atoms drives the spatial orientation of the P1 and P2 groups. The inhibitors presented here have been synthesized and isolated both as S,R,R and S,S,S isomers, with only the former retaining significant inhibitory properties, which confirms previous observation by Guay et al.³³ A large number of the inhibitors presented here has been synthesized and isolated both as S,R,R and S,S,S isomers. The best inhibitory effects were associated with the S,R,R forms. However, the magnitude of the effect strongly varied with different side chains in P2, as illustrated. Guay et al. also reported that the S, R, R isomers were more potent than the S,S,S isomers.³³

The crystal structures of CatC with a cyanamide-based inhibitor³⁵ and nitrile inhibitors have been reported.³² The 3D structures of CatC in complex with the cyclopropyl compounds **5a**, **9a** or **13a** as reported here, confirmed the covalent binding of the nitrile group with cysteine 234 and showed that substituted biphenyl moieties were oriented towards the exclusion domain and were close to the proline at position 3. Because of the solvent-exposure of the S1 subsite at the surface of CatC, P1 residues bearing aliphatic, hydrophobic, polar, basic or acidic natural amino acid side chains can be accommodated. Thus, a biphenyl group and its derivatives with *p*-trifluoromethyl (compound **5a**), 4-methylpiperazin-1-yl)-[1,2,4]triazolo[1,5-a]pyridin-6-yl)phenyl (compound **7a**) and 4'-(4-methylpiperazin-1-

ylsulfonyl (compound **8a**) can be accommodated at P1. However, long aliphatic side chains added to the biphenyl moiety directed towards proline 3 might not be tolerated at the P1 position. The S2 subsite of CatC displays the shape of a deep pocket filled with a chloride ion at the bottom.^{25, 27} The P2 side chain is of great importance to inhibitor's potency.^{31, 33} Therefore, we tested different side chains at P2 to tentatively improve the potency of **IcatC_{XPZ-01}**. We observed that 2-thienylmethyl or 2-furanylmethyl is optimal at P2, as also reported by Guay et al.³³ However, from the profiling data (*e.g.* metabolic stability) generated here, **IcatC_{XPZ-01}** with an ethyl group at P2 was more suitable for *in vivo* experiments.

IcatC_{XPZ-01} was identified to be selective over cathepsine H, K, L, S, NSPs and DPP4.¹⁸ We ascertained that **IcatC_{XPZ-01}** retained similar inhibitory properties towards human and rodent CatC. Doyle et al. reported an accurate species crossover potency for the CatC inhibitor AZD7986.³⁷ We have evaluated the *in vivo* efficacy of **IcatC_{XPZ-01}**, first by studying its distribution in mice. Analysis of the PK profile indicated that **IcatC_{XPZ-01}** accumulated in the bone marrow and reached a sufficiently high level for CatC inhibition by two administrations 4.8 mg/kg per day. NSPs activities in bone marrow cell extracts remained substantially and dose dependently reduced after twice-daily administration of **IcatC_{XPZ-01}**. The reduction of CatG activity is more pronounced than found for NE/PR3. Adkinson and coworkers used the same chromogenic substrates⁵ as used in the present study for measuring activity in bone marrow lysates from CatC^{-/-}, NE^{-/-} and CatG^{-/-} mice. In this study, CatG activity was totally abolished while a residual activity was found when using the NE/PR3 substrate. This residual activity comprising 15-30% of activity found for wild-type mice was most likely attributable to irrelevant proteases present in the extracts. Lack of total specificity of the substrate for NE/PR3 is also supposed to be the explanation for the difference between the degrees of reduction of CatG compared to NE/PR3 in the present study. The results showed that **IcatC_{XPZ-01}** was able to reduce activation of bone marrow NE and CatG in a dose

dependent manner *in vivo*. Based on CatG activity the reduction was in the order of 60-70% for the lowest dose (1.2 mg/kg) and 75-90% for the highest dose 4.8 mg/kg. The reduction was persistent for at least 24 hours after the last dose. Doyle et al. reported also almost total inhibition of NSPs after CatC inhibitor AZD7986 administration in mice.³⁷

Adkison and coworkers showed that CatC^{-/-} mice were protected against the development of experimental arthritis.⁵ This effect was attributed to the inactivation of NSPs as NE/CatG double knock-out mice were also resistant to arthritis. We aimed at demonstrating experimentally how this resistance observed in CatC^{-/-} mice can be obtained by pharmacological targeting of CatC. The efficacy of **IcatC_{XPZ-01}** was evaluated in a mouse model of CAIA. The cocktail of arthritogenic monoclonal antibodies against collagen type II in combination with a boost of LPS accelerated the onset of an acute arthritis within 48 h after LPS injection and 5 days after antibody administration. Subcutaneous administration of **IcatC_{XPZ-01}** in this CAIA model showed a statistically significant and sustained reductions in total arthritis scores, as well as rear paw arthritis scores and rear paw thickness. Even though the two doses, 1.2 mg/kg and 4.8 mg/kg, resulted in statistically significant differences in active NSP levels, no statistically significant difference in the anti-arthritic activity was found between the two doses. In other words, 60-70% reduction in NSP's had the same anti-arthritic effect as 75-90% reduction. However, it is not possible based on this particular disease model and the obtained degrees of reduction to assess how much NSP reduction is sufficient or optimal in order to get an anti-inflammatory effect in general.

A series of novel dipeptidyl cyclopropyl nitrile inhibitors of CatC with characteristics suitable for *in vivo* experiments have been synthesized. **IcatC_{XPZ-01}** ((S)-2-amino-N-((1R,2R)-1-cyano-2-(4'-(4-methylpiperazin-1-ylsulfonyl)biphenyl-4-yl)cyclopropyl)butanamide)) (Patent Pub. No.: WO/2012/130299) has been identified as a potent and cell permeable CatC inhibitor that showed non-significant inhibition of CYP450 enzymes and hERG channel.

IcatC_{XPZ-01} is resistant to hydrolytic degradation and displays a suitable metabolic stability. We demonstrated that **IcatC_{XPZ-01}** by preventing maturation of NSPs, exhibited a potent anti-arthritic activity in a mouse model of rheumatoid arthritis. These results strongly support the therapeutic interest of continuous pharmacological blockade of CatC in NSPs driven inflammatory diseases.

Financial support

This work was supported by Unizyme, the “Ministère de l'Enseignement Supérieur et de la Recherche”, the “Région Centre” (Project BPCO-Lyse) and “National Science Center Poland (UMO 2014/15/B/ST5/05311) granted to Adam Lesner.

Author information

Corresponding Authors

Brice Korkmaz, Tel: +33 2 47 36 63 86, e-mail: brice.korkmaz@inserm.fr

John Pedersen, Tel: +45 2049 7831, e-mail: jp@neuprozyme.com

Authorship Contributions

Brice Korkmaz and John Pedersen supervised the work.

Conni Lauritzen, John Pedersen and Brice Korkmaz participated in the research design. Conni Lauritzen, Artur Gieldon, Maria Håkansson, Derek Logan and Brice Korkmaz conducted the experiments. Brice Korkmaz, John Pedersen, Conni Lauritzen, Adam Lesner, Magdalena Wysocka, Francis Gauthier, and Dieter E. Jenne performed data analyses. Brice Korkmaz wrote the manuscript. Brice Korkmaz, Adam Lesner, Magdalena Wysocka and Artur Gieldon prepared figures. All authors contributed to the writing and revision processes of the manuscript.

Disclosure of conflicts of interest

John Pedersen and Conni Lauritzen are employed by Neuprozyme Therapeutics Aps who aims to develop therapeutic inhibitors of CatC in the field of chronic inflammatory or auto-immune diseases. Neuprozyme Therapeutics Aps declares no conflict of interest. Derek Logan and Maria Håkansson are employees of SARomics Biostructures AB who performed the crystal structure determinations under contract to Unizyme Laboratories A/S which has a collaboration with Neuprozyme Therapeutics Aps regarding development of inhibitors of CatC. John Pedersen and Conni Lauritzen are also employees of Unizyme Laboratories A/S, which declares no conflict of interest. SARomics Biostructures AB has no financial interest in this work. The academic authors declare no competing interests. The patent application for IcatC_{XPZ-01} (Patent Pub. No. WO/2012/130299) has been abandoned.

Acknowledgments

Brice Korkmaz acknowledges the “Alexandre von Humboldt Foundation”. We would like to thank the staffs at PepTech Inc. (Burlington, MA, USA), MD Biosciences (Glasgow, UK). We are also grateful to Prof. Gilles Lalmanach and Dr Mustapha Si-Tahar for their critical reading of the manuscript.

Accession codes

The coordinates and the structure factor amplitudes for CatC complexes with compound **5a**, **9a** and **13a** have been deposited with the Protein Data Bank (<http://www.rcsb.org>) with the following accession codes: 6IC6 (compound **5a**), 6IC7 (compound **9a**) and 6IC5 (compound **13a**). The authors will release the atomic coordinates upon article publication.

References

- (1) Brown, G. R.; McGuire, M. J.; Thiele, D. L. Dipeptidyl peptidase I is enriched in granules of in vitro- and in vivo-activated cytotoxic T lymphocytes. *J. Immunol.* **1993**, 150, 4733-4742.
- (2) Korkmaz, B.; Caughey, G. H.; Chapple, I.; Gauthier, F.; Hirschfeld, J.; Jenne, D. E.; Kettritz, R.; Lalmanach, G.; Lamort, A. S.; Lauritzen, C.; Legowska, M.; Lesner, A.; Marchand-Adam, S.; McKaig, S. J.; Moss, C.; Pedersen, J.; Roberts, H.; Schreiber, A.; Seren, S.; Thakker, N. S. Therapeutic targeting of cathepsin C: from pathophysiology to treatment. *Pharmacol. Ther.* **2018**.
- (3) McGuire, M. J.; Lipsky, P. E.; Thiele, D. L. Generation of active myeloid and lymphoid granule serine proteases requires processing by the granule thiol protease dipeptidyl peptidase I. *J. Biol. Chem.* **1993**, 268, 2458-2467.
- (4) Tran, T. V.; Ellis, K. A.; Kam, C. M.; Hudig, D.; Powers, J. C. Dipeptidyl peptidase I: importance of progranzyme activation sequences, other dipeptide sequences, and the N-terminal amino group of synthetic substrates for enzyme activity. *Arch. Biochem. Biophys.* **2002**, 403, 160-170.
- (5) Adkison, A. M.; Raptis, S. Z.; Kelley, D. G.; Pham, C. T. Dipeptidyl peptidase I activates neutrophil-derived serine proteases and regulates the development of acute experimental arthritis. *J. Clin. Invest.* **2002**, 109, 363-371.
- (6) Pham, C. T.; Ivanovich, J. L.; Raptis, S. Z.; Zehnbauser, B.; Ley, T. J. Papillon-Lefevre syndrome: correlating the molecular, cellular, and clinical consequences of cathepsin C/dipeptidyl peptidase I deficiency in humans. *J. Immunol.* **2004**, 173, 7277-7281.
- (7) Perera, N. C.; Wiesmuller, K. H.; Larsen, M. T.; Schacher, B.; Eickholz, P.; Borregaard, N.; Jenne, D. E. NSP4 is stored in azurophil granules and released by activated neutrophils as active endoprotease with restricted specificity. *J. Immunol.* **2013**, 191, 2700-2707.
- (8) Cowland, J. B.; Borregaard, N. Granulopoiesis and granules of human neutrophils. *Immunol. Rev.* **2016**, 273, 11-28.
- (9) Jenne, D. E.; Kuhl, A. Production and applications of recombinant proteinase 3, Wegener's autoantigen: problems and perspectives. *Clin. Nephrol.* **2006**, 66, 153-159.
- (10) Korkmaz, B.; Horwitz, M. S.; Jenne, D. E.; Gauthier, F. Neutrophil elastase, proteinase 3, and cathepsin G as therapeutic targets in human diseases. *Pharmacol. Rev.* **2010**, 62, 726-759.
- (11) Korkmaz, B.; Moreau, T.; Gauthier, F. Neutrophil elastase, proteinase 3 and cathepsin G: physicochemical properties, activity and physiopathological functions. *Biochimie* **2008**, 90, 227-242.
- (12) Papillon, M. M.; Lefèvre, P. 2 cases of symmetrically, familiarly palmar and plantar hyperkeratosis (Meleda disease) within brother and sister combined with severe dental alterations in both cases. *Soc Franc Dermat Syph* **1924**, 31, 82-84.
- (13) Toomes, C.; James, J.; Wood, A. J.; Wu, C. L.; McCormick, D.; Lench, N.; Hewitt, C.; Moynihan, L.; Roberts, E.; Woods, C. G.; Markham, A.; Wong, M.; Widmer, R.; Ghaffar, K. A.; Pemberton, M.; Hussein, I. R.; Temtamy, S. A.; Davies, R.; Read, A. P.; Sloan, P.; Dixon, M. J.; Thakker, N. S. Loss-of-function mutations in the cathepsin C gene result in periodontal disease and palmoplantar keratosis. *Nat. Genet.* **1999**, 23, 421-424.
- (14) Hart, T. C.; Hart, P. S.; Bowden, D. W.; Michalec, M. D.; Callison, S. A.; Walker, S. J.; Zhang, Y.; Firatli, E. Mutations of the cathepsin C gene are responsible for Papillon-Lefevre syndrome. *J. Med. Genet.* **1999**, 36, 881-887.

- (15) Gorlin, R. J.; Sedano, H.; Anderson, V. E. The Syndrome of Palmar-Plantar Hyperkeratosis and Premature Periodontal Destruction of the Teeth. A Clinical and Genetic Analysis of the Papillon-Lefevre Syndrome. *J. Pediatr.* **1964**, 65, 895-908.
- (16) Haneke, E. The Papillon-Lefevre syndrome: keratosis palmoplantaris with periodontopathy. Report of a case and review of the cases in the literature. *Hum. Genet.* **1979**, 51, 1-35.
- (17) Dhanrajani, P. J. Papillon-Lefevre syndrome: clinical presentation and a brief review. *Oral Surg. Oral Med. Oral Pathol. Oral Radiol. Endod.* **2009**, 108, e1-7.
- (18) Guarino, C.; Hamon, Y.; Croix, C.; Lamort, A. S.; Dallet-Choisy, S.; Marchand-Adam, S.; Lesner, A.; Baranek, T.; Viaud-Massuard, M. C.; Lauritzen, C.; Pedersen, J.; Heuze-Vourch, N.; Si-Tahar, M.; Firatli, E.; Jenne, D. E.; Gauthier, F.; Horwitz, M. S.; Borregaard, N.; Korkmaz, B. Prolonged pharmacological inhibition of cathepsin C results in elimination of neutrophil serine proteases. *Biochem. Pharmacol.* **2017**, 131, 52-67.
- (19) Sorensen, O. E.; Clemmensen, S. N.; Dahl, S. L.; Ostergaard, O.; Heegaard, N. H.; Glenthoj, A.; Nielsen, F. C.; Borregaard, N. Papillon-Lefevre syndrome patient reveals species-dependent requirements for neutrophil defenses. *J. Clin. Invest.* **2014**, 124, 4539-4548.
- (20) Seren, S.; Rashed Abouzaid, M.; Eulenberg-Gustavus, C.; Hirschfeld, J.; Nasr Soliman, H.; Jerke, U.; N'Guessan, K.; Dallet-Choisy, S.; Lesner, A.; Lauritzen, C.; Schacher, B.; Eickholz, P.; Nagy, N.; Szell, M.; Croix, C.; Viaud-Massuard, M. C.; Al Farraj Aldosari, A.; Ragunatha, S.; Ibrahim Mostafa, M.; Giampieri, F.; Battino, M.; Cornillier, H.; Lorette, G.; Stephan, J. L.; Goizet, C.; Pedersen, J.; Gauthier, F.; Jenne, D. E.; Marchand-Adam, S.; Chapple, I. L.; Kettritz, R.; Korkmaz, B. Consequences of cathepsin C inactivation for membrane exposure of proteinase 3, the target antigen in autoimmune vasculitis. *J. Biol. Chem.* **2018**, 293, 12415-12428.
- (21) Korkmaz, B.; Lesner, A.; Letast, S.; Mahdi, Y. K.; Jourdan, M. L.; Dallet-Choisy, S.; Marchand-Adam, S.; Kellenberger, C.; Viaud-Massuard, M. C.; Jenne, D. E.; Gauthier, F. Neutrophil proteinase 3 and dipeptidyl peptidase I (cathepsin C) as pharmacological targets in granulomatosis with polyangiitis (Wegener granulomatosis). *Semin. Immunopathol.* **2013**, 35, 411-421.
- (22) Hu, Y.; Pham, C. T. Dipeptidyl peptidase I regulates the development of collagen-induced arthritis. *Arthritis Rheum.* **2005**, 52, 2553-2558.
- (23) Dahl, S. W.; Halkier, T.; Lauritzen, C.; Dolenc, I.; Pedersen, J.; Turk, V.; Turk, B. Human recombinant pro-dipeptidyl peptidase I (cathepsin C) can be activated by cathepsins L and S but not by autocatalytic processing. *Biochemistry* **2001**, 40, 1671-1678.
- (24) Lauritzen, C.; Pedersen, J.; Madsen, M. T.; Justesen, J.; Martensen, P. M.; Dahl, S. W. Active recombinant rat dipeptidyl aminopeptidase I (cathepsin C) produced using the baculovirus expression system. *Protein Expr Purif* **1998**, 14, 434-442.
- (25) Turk, D.; Janjic, V.; Stern, I.; Podobnik, M.; Lamba, D.; Dahl, S. W.; Lauritzen, C.; Pedersen, J.; Turk, V.; Turk, B. Structure of human dipeptidyl peptidase I (cathepsin C): exclusion domain added to an endopeptidase framework creates the machine for activation of granular serine proteases. *EMBO J.* **2001**, 20, 6570-6582.
- (26) Turk, V.; Stoka, V.; Vasiljeva, O.; Renko, M.; Sun, T.; Turk, B.; Turk, D. Cysteine cathepsins: from structure, function and regulation to new frontiers. *Biochim. Biophys. Acta.* **2012**, 1824, 68-88.
- (27) Molgaard, A.; Arnau, J.; Lauritzen, C.; Larsen, S.; Petersen, G.; Pedersen, J. The crystal structure of human dipeptidyl peptidase I (cathepsin C) in complex with the inhibitor Gly-Phe-CHN₂. *Biochem. J.* **2007**, 401, 645-650.
- (28) Schechter, I.; Berger, A. On the size of the active site in proteases. I. Papain. *Biochem. Biophys. Res. Commun.* **1967**, 27, 157-162.

- (29) Dolenc, I.; Turk, B.; Pungercic, G.; Ritonja, A.; Turk, V. Oligomeric structure and substrate induced inhibition of human cathepsin C. *J. Biol. Chem.* **1995**, 270, 21626-21631.
- (30) Cigic, B.; Pain, R. H. Location of the binding site for chloride ion activation of cathepsin C. *Eur. J. Biochem.* **1999**, 264, 944-951.
- (31) Bondebjerg, J.; Fuglsang, H.; Valeur, K. R.; Pedersen, J.; Naerum, L. Dipeptidyl nitriles as human dipeptidyl peptidase I inhibitors. *Bioorg. Med. Chem. Lett.* **2006**, 16, 3614-3617.
- (32) Furber, M.; Tiden, A. K.; Gardiner, P.; Mete, A.; Ford, R.; Millichip, I.; Stein, L.; Mather, A.; Kinchin, E.; Luckhurst, C.; Barber, S.; Cage, P.; Sanganee, H.; Austin, R.; Chohan, K.; Beri, R.; Thong, B.; Wallace, A.; Oreffo, V.; Hutchinson, R.; Harper, S.; Debreczeni, J.; Breed, J.; Wissler, L.; Edman, K. Cathepsin C inhibitors: property optimization and identification of a clinical candidate. *J. Med. Chem.* **2014**, 57, 2357-2367.
- (33) Guay, D.; Beaulieu, C.; Truchon, J. F.; Jagadeeswar Reddy, T.; Zamboni, R.; Bayly, C. I.; Methot, N.; Rubin, J.; Ethier, D.; David Percival, M. Design and synthesis of dipeptidyl nitriles as potent, selective, and reversible inhibitors of cathepsin C. *Bioorg. Med. Chem. Lett.* **2009**, 19, 5392-5396.
- (34) Laine, D. I.; Busch-Petersen, J. Inhibitors of cathepsin C (dipeptidyl peptidase I). *Expert. Opin. Ther. Pat.* **2010**, 20, 497-506.
- (35) Laine, D.; Palovich, M.; McClelland, B.; Petitjean, E.; Delhom, I.; Xie, H.; Deng, J.; Lin, G.; Davis, R.; Jolit, A.; Nevins, N.; Zhao, B.; Villa, J.; Schneck, J.; McDevitt, P.; Midgett, R.; Kmetz, C.; Umbrecht, S.; Peck, B.; Davis, A. B.; Bettoun, D. Discovery of novel cyanamide-based inhibitors of cathepsin C. *ACS Med. Chem. Lett.* **2011**, 2, 142-147.
- (36) Miller, B. E.; Mayer, R. J.; Goyal, N.; Bal, J.; Dallow, N.; Boyce, M.; Carpenter, D.; Churchill, A.; Heslop, T.; Lazaar, A. L. Epithelial desquamation observed in a phase I study of an oral cathepsin C inhibitor (GSK2793660). *Br J Clin Pharmacol* **2017**, 83, 2813-2820.
- (37) Doyle, K.; Lonn, H.; Kack, H.; Van de Poel, A.; Swallow, S.; Gardiner, P.; Connolly, S.; Root, J.; Wikell, C.; Dahl, G.; Stenvall, K.; Johannesson, P. Discovery of Second Generation Reversible Covalent DPP1 Inhibitors Leading to an Oxazepane Amidoacetonitrile Based Clinical Candidate (AZD7986). *J. Med. Chem.* **2016**, 59, 9457-9472.
- (38) Methot, N.; Guay, D.; Rubin, J.; Ethier, D.; Ortega, K.; Wong, S.; Normandin, D.; Beaulieu, C.; Reddy, T. J.; Riendeau, D.; Percival, M. D. In vivo inhibition of serine protease processing requires a high fractional inhibition of cathepsin C. *Mol. Pharmacol.* **2008**, 73, 1857-1865.
- (39) Methot, N.; Rubin, J.; Guay, D.; Beaulieu, C.; Ethier, D.; Reddy, T. J.; Riendeau, D.; Percival, M. D. Inhibition of the activation of multiple serine proteases with a cathepsin C inhibitor requires sustained exposure to prevent pro-enzyme processing. *J. Biol. Chem.* **2007**, 282, 20836-20846.
- (40) Guay, D.; Beaulieu, C.; Percival, M. D. Therapeutic utility and medicinal chemistry of cathepsin C inhibitors. *Curr. Top. Med. Chem.* **2010**, 10, 708-716.
- (41) Lebedev, A. A.; Young, P.; Isupov, M. N.; Moroz, O. V.; Vagin, A. A.; Murshudov, G. N. J. Ligand: a graphical tool for the CCP4 template-restraint library. *Acta Crystallogr D Biol Crystallogr* **2012**, 68, 431-440.
- (42) Winn, M. D.; Ballard, C. C.; Cowtan, K. D.; Dodson, E. J.; Emsley, P.; Evans, P. R.; Keegan, R. M.; Krissinel, E. B.; Leslie, A. G.; McCoy, A.; McNicholas, S. J.; Murshudov, G. N.; Pannu, N. S.; Potterton, E. A.; Powell, H. R.; Read, R. J.; Vagin, A.; Wilson, K. S. Overview of the CCP4 suite and current developments. *Acta Crystallogr D Biol Crystallogr* **2011**, 67, 235-242.
- (43) Murshudov, G. N.; Skubak, P.; Lebedev, A. A.; Pannu, N. S.; Steiner, R. A.; Nicholls, R. A.; Winn, M. D.; Long, F.; Vagin, A. A. REFMAC5 for the refinement of macromolecular crystal structures. *Acta Crystallogr D Biol Crystallogr* **2011**, 67, 355-367.

- (44) Emsley, P.; Lohkamp, B.; Scott, W. G.; Cowtan, K. Features and development of Coot. *Acta Crystallogr D Biol Crystallogr* **2010**, 66, 486-501.
- (45) Winn, M. D.; Isupov, M. N.; Murshudov, G. N. Use of TLS parameters to model anisotropic displacements in macromolecular refinement. *Acta Crystallogr D Biol Crystallogr* **2001**, 57, 122-133.
- (46) Frizler, M.; Stirnberg, M.; Sisay, M. T.; Gutschow, M. Development of nitrile-based peptidic inhibitors of cysteine cathepsins. *Curr. Top. Med. Chem.* **2010**, 10, 294-322.

Figure legends

Figure 1: Illustration of neutrophil serine protease zymogens activation by CatC in physiological condition (*left*) and their elimination in presence of a CatC inhibitor (*right*).

Figure 2: Three examples of nitrile-based inhibitors of CatC reported in the literature compared to compound 8a (IcatC_{XPZ-01}). Chemical structures of Abu-Bip-CN³¹ (identical to compound 1) (A), AZD7986³⁷ (B), a dipeptidyl cyclopropyl nitrile³⁹ (C), and compound 8a (IcatC_{XPZ-01}). ^a AZD7986 was obtained from MedChemExpress, Cat. No.: HY-101056, ^b synthesized as in Ref³⁹. Recombinant mature human CatC was used for IC₅₀ CatC determination in an assay based on Gly-Phe-pNA (*para*-nitroanilide) as substrate. The human pro-monocytic leukemia cell line U937 containing endogenous CatC was grown in the presence of CatC inhibitors in order to determine the downstream effect on the activity of the CatC activated proteases. IC₅₀ U937 was determined in cell lysates using the substrate MeOSuc-AAPV-pNA. The listed potencies are determined in identical assay setups as used for the values in Table 3.

Figure 3: Synthetic schema for the synthesis of compound 8a and compound 8b. (a) 4-bromobenzaldehyde, MeOH, p-toluenesulfonyl hydrazide, RT, 30 min, next 0 °C; N'-(4-bromobenzylidene)-4-methylbenzenesulfonohydrazide (II). (b) II, THF, -78 °C, BuLi, -78 °C, 1 h. (c) methyl 2-(tert-butyloxycarbonylamino)acrylate (I) (0.16 mol), benzyltriethylammonium chloride, ClFeTPP, toluene, 50 °C under N₂ protection, 4 days; (1*R*,2*R*)- and (1*S*,2*S*)-methyl-2-(4-bromophenyl)-1-(tert-butyloxycarbonylamino)cyclopropanecarboxylate (IIIa and IIIb). (d) Pd(PPh₃)₄, 1-(4-bromophenyl sulfonyl)-4-methylpiperazine (1), pinacolatodiboron, K₂CO₃, toluene, heated,

12 h; 1-methyl-4-[4-(4,4,5,5-tetramethyl-1,3,2-dioxaborolan-2-yl)phenylsulfonyl]piperazine (2). (e) $\text{PdCl}_2(\text{dppf})_2$, **2**, **IIIa** and **IIIb**, 2 M Na_2CO_3 (aq. solution), 1,4-dioxane, 12 h under nitrogen protection; (1*R*,2*R*) and (1*S*,2*S*)-methyl 1-(tert-butyloxycarbonylamino)-2-[4'-(4-methyl-piperazin-1-yl-sulfonyl)biphenyl-4-yl]cyclopropanecarboxylate (**3a**) and (**3b**). (f) **3a** and **3b**, THF, 6 N HCl, 40 °C, 4 h; (1*R*,2*R*) and (1*S*,2*S*)-methyl-1-amino-2-[4'-(4-methylpiperazin-1-yl-sulfonyl)-biphenyl-4-yl]-cyclopropanecarboxylate (**4a**) and (**4b**). (g) Boc-Abu-OH, NMM, CH_2Cl_2 , 0 °C, ethyl chloroformate, 0 °C, 1 h, **4a** and **4b**, CH_2Cl_2 , RT, 12 h. (h) chiral column, (1*R*,2*R*)-methyl-(*S*)-2-(tert-butyloxycarbonylamino)butanamido)-2-(4'-(4-methylpiperazin-1-ylsulfonyl)biphenyl-4-yl)cyclopropanecarboxylate (**5a**), (1*S*,2*S*)-methyl-((*S*)-2-(tert-butyloxycarbonylamino)butanamido)-2-(4'-(4-methyl-piperazin-1-ylsulfonyl)biphenyl-4-yl)cyclopropanecarboxylate (**5b**). (i) $\text{LiOH}\cdot\text{H}_2\text{O}$, **5a** or **5b**, THF/ H_2O , RT, 3 h. (j) CH_2Cl_2 , NMM, 0 °C, ethyl chloroformate, 0 °C, 1 h. (k) Ammonia, RT, 12 h; tert-butyloxycarbonylamino-(*S*)-1-((1*R*,2*R*)-1-carbamoyl-2-(4'-(4-methylpiperazin-1-yl-sulfonyl)biphenyl-4-yl)cyclopropylamino)-1-oxobutan-2-ylcarbamate (**6a**); tert-butyloxycarbonylamino-(*S*)-1-((1*S*,2*S*)-1-carbamoyl-2-(4'-(4-methylpiperazin-1-yl-sulfonyl)biphenyl-4-yl)cyclopropylamino)-1-oxobutan-2-ylcarbamate (**6b**). (l) **6a** (0.92 mmol), DMF, cyanuric chloride, RT, 4 h; Boc-(*S*)-2-amino-N-((1*R*,2*R*)-1-cyano-2-(4'-(4-methylpiperazin-1-ylsulfonyl)biphenyl-4-yl)cyclopropyl)butanamide (Boc-compound **8a**) (150 mg). (m) Boc-compound **8a**, HCOOH , RT, 4 h, NaHCO_3 in water; (*S*)-2-amino-N-((1*R*,2*R*)-1-cyano-2-(4'-(4-methylpiperazin-1-ylsulfonyl)biphenyl-4-yl)cyclopropyl)butanamide (compound **8a**). (n) **6b**, DMF, cyanuric chloride, RT, 4 h; Boc-(*S*)-2-amino-N-((1*S*,2*S*)-1-cyano-2-(4'-(4-methyl-piperazin-1-ylsulfonyl)biphenyl-4-yl)cyclopropyl)butanamide (Boc-compound **8b**). (o) Boc-compound **8b**, HCOOH , RT, 4 h, NaHCO_3 in water. The synthetic scheme for compound **8a** has been adapted for the synthesis of huge amount in our previous publication.¹⁸

Figure 4: X-ray structures of compounds 5a (A) or compound 9a (B) in complex with CatC in standard orientation of papain-like cysteine proteases. (*Top*) The overall binding of the backbone of the two inhibitors is identical and differ only at their extremities, on the protein surface and deep in the binding pocket, respectively. Both inhibitors make the same four hydrogen bonds to protein main- and side-chain atoms (Asp1, Cys234, Gly277, Asn380). The carbon atoms of the inhibitors are shown in yellow. The oxygen, nitrogen, sulfur and fluor atoms are colored in red, blue, orange and turquoise, respectively. (*Bottom*) Solvent-accessible surfaces of CatC complexed with the inhibitor. The carbon, oxygen, nitrogen, sulfur atoms of CatC are colored in gray, red, blue and yellow, respectively.

Figure 5: Rotameric analysis of 4-methylpiperazin, 4-methylpiperazin-1-yl)-[1,2,4]triazolo[1,5-a]pyridin-6-yl)phenyl and 4'-(4-methylpiperazin-1-ylsulfonyl) attached to the biphenyl moiety of compound 5a crystalized in the complex with CatC. The coordinates of CatC complex with compound 9a (PDB ID code: 6IC7) was used for molecular modeling.

Figure 6: Pharmacokinetic profile of IcatC_{XPZ-01} in mice. **A)** Average plasma concentration versus time profiles of **IcatC_{XPZ-01}** following subcutaneous administration in mice at 4.8 mg/kg. **B)** Bone marrow concentration versus time profile of **IcatC_{XPZ-01}** following subcutaneous administration in mice at 4.8 mg/kg. Mice in group 2 received two separate subcutaneous doses of **IcatC_{XPZ-01}** (4.8 mg/kg) at time 0, and again at 12 h post 1st dose. Concentrations of **IcatC_{XPZ-01}** were determined by LC-MS/MS in each separate plasma sample or in a pool of the three bone marrow samples.

Figure 7: Schematic depiction illustrating the arthritis induction and the treatments

administration in mice. Mice were treated subcutaneously twice daily with vehicle (negative control GROUP 1, n=13) or **IcatC_{XPZ-01}** at 1.2 mg/kg (GROUP 2, n=12) or 4.8 mg/kg (GROUP 3, n=12) from study day -14 to study day 11 (26 days in total). All mice were subjected on day 0 of the study (*study commencement*) to a tail vein injection of an arthritogenic monoclonal anti-collagen II antibody cocktail. Three days after mAb administration, all animals were exposed to LPS by a single intraperitoneal injection. Enbrel, was administered as a positive control intraperitoneally, once a day, from study day 0 to study day 11 (GROUP 4, n=10).

Figure 8: Proteolytic activities of NE/PR3 and CatG in bone marrow cells.

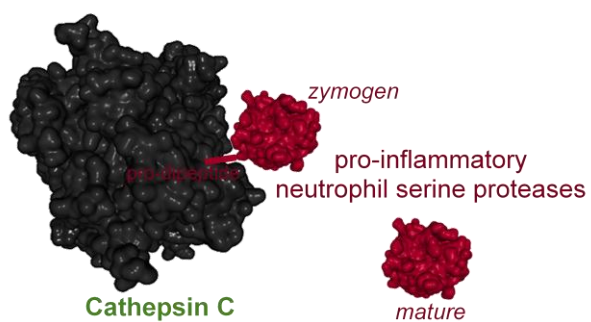
At termination of the CAIA study bone marrow was isolated at 1, 12, and 24 h after the last dose and proteolytic activities were measured in cell extracts. Data represents 4 samples from each group. Asterisks indicate significant differences: * $P < 0.05$, ** $P < 0.01$, *** $P < 0.001$, **** $P < 0.0001$ (Student's *t*-test). the data in the figure was from bone marrow

Figure 9: Anti-arthritic activity evaluation of IcatC_{XPZ-01} in a mouse model of

rheumatoid arthritis induced by anti-collagen antibodies. A) Mean total arthritis scores determined from day 0 to day 12. Graph shows mean \pm SEM. *, represents Enbrel treated group significantly different to the vehicle treated group; †, represents **IcatC_{XPZ-01}** 1.2 mg/kg treated group significantly different to the vehicle treated group; §, represents **IcatC_{XPZ-01}** 4.8 mg/kg treated group significantly different to the vehicle treated group. **B)** Mean rear paw arthritis scores determined from day 0 to day 12. Graph shows mean \pm SEM. *, represents Enbrel treated group significantly different to the vehicle treated group; †, represents **IcatC_{XPZ-01}** 1.2 mg/kg treated group significantly different to the vehicle treated group; §,

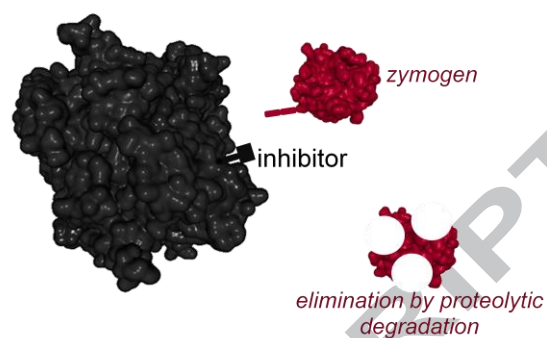
represents **IcatC_{XPZ-01}** 4.8 mg/kg treated group significantly different to the vehicle treated group. C) Mean rear paw thickness (mm) determined from day 0 to day 12. Graph shows mean \pm SEM. *, represents Enbrel treated group significantly different to the vehicle treated group; †, represents **IcatC_{XPZ-01}** 1.2 mg/kg treated group significantly different to the vehicle treated group; §, represents **IcatC_{XPZ-01}** 4.8 mg/kg treated group significantly different to the vehicle treated group.

PHYSIOLOGICAL CONDITION

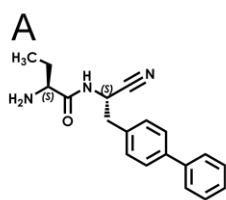


ZYMOGEN ACTIVATION BY REMOVING
N-TERMINAL PRO-DIPEPTIDE

PHARMACOLOGICAL INTERVENTION

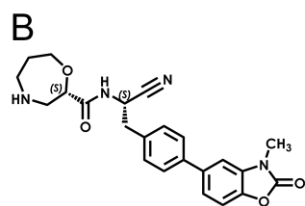


INHIBITION OF CATHEPSIN C RESULTING IN
ELIMINATION OF ZYMOGENS



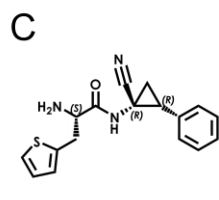
Abu-Bip-CN
(Compound 1)

- IC_{50} CatC = 8 nM
- IC_{50} U937 = no inhibition
- Not stable in plasma



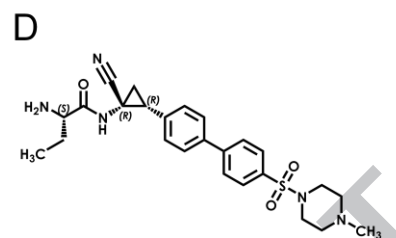
AZD7986^a

- IC_{50} CatC = 22 nM
- IC_{50} U937 = 30 nM
- Stable in plasma



**Dipeptidyl cyclopropyl
nitrile^b**

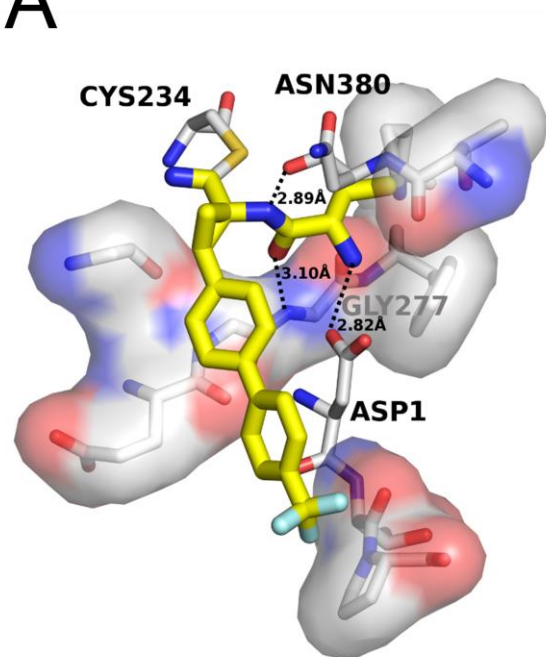
- IC_{50} CatC = 48 nM
- IC_{50} U937 = ~650 nM
- Stable in plasma



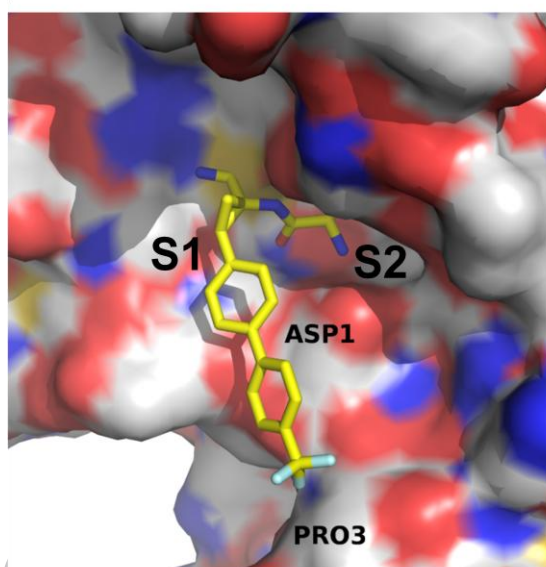
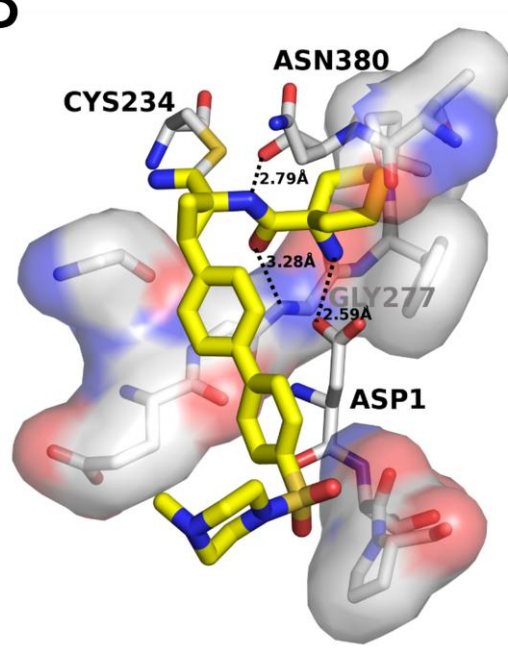
Compound 8a
(IcatC_{XP2-01})

- IC_{50} CatC = 15 nM
- IC_{50} U937 = 6 nM
- Stable in plasma

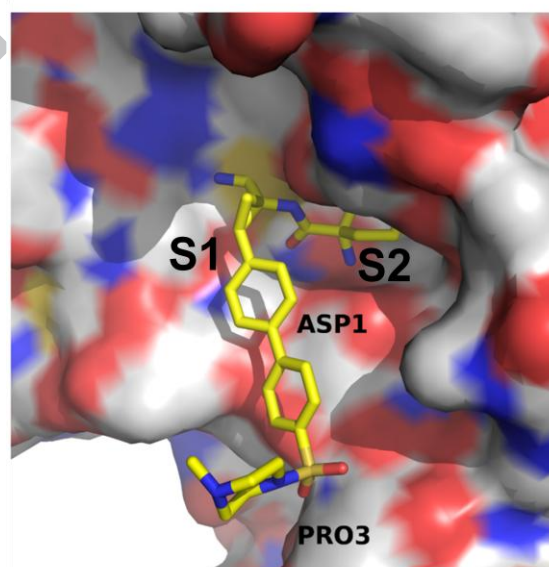
A



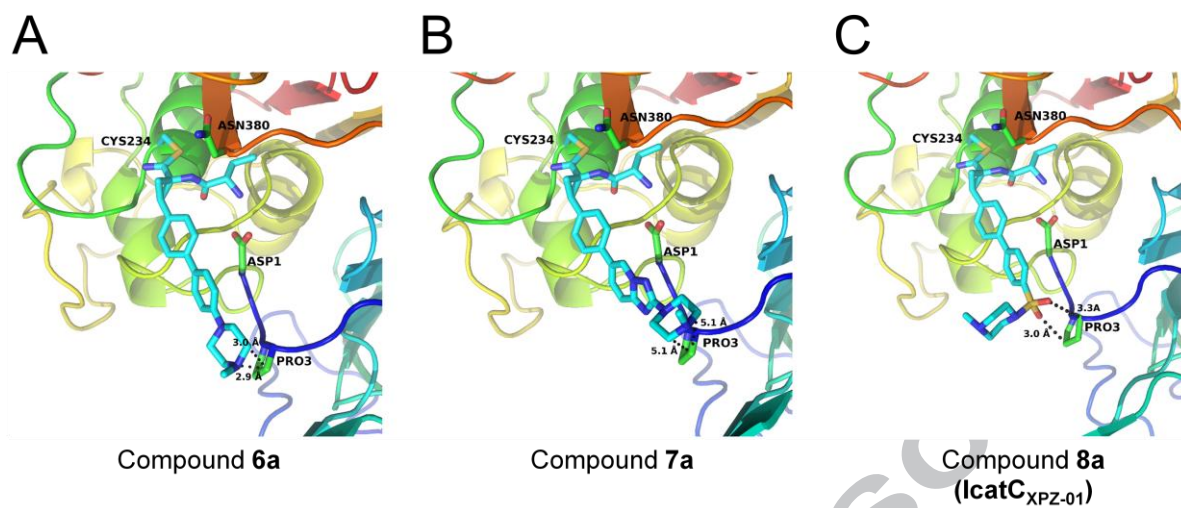
B

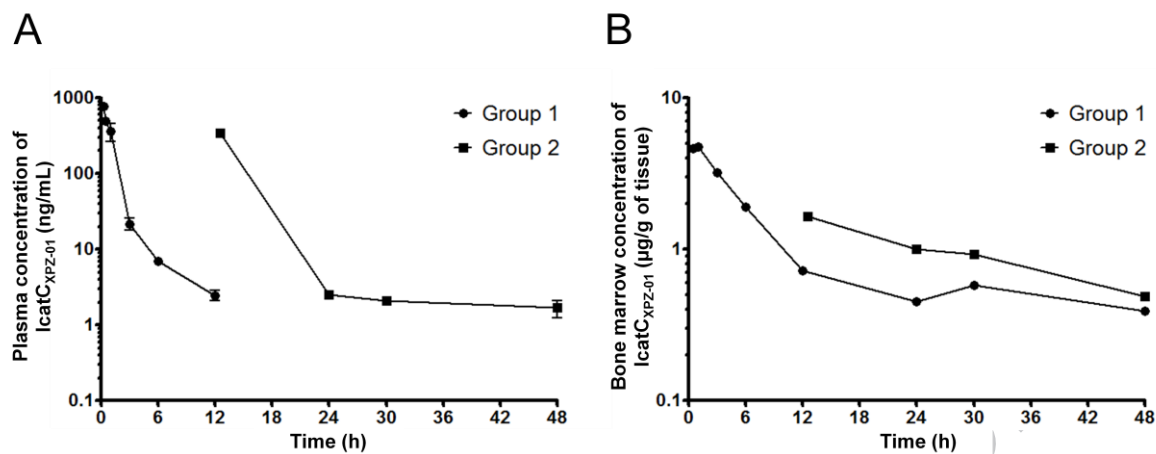


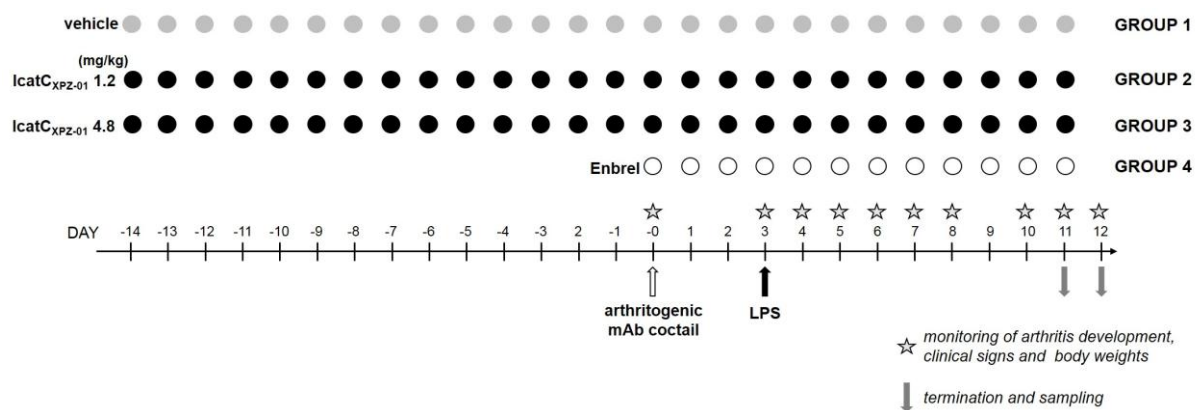
Compound 5a

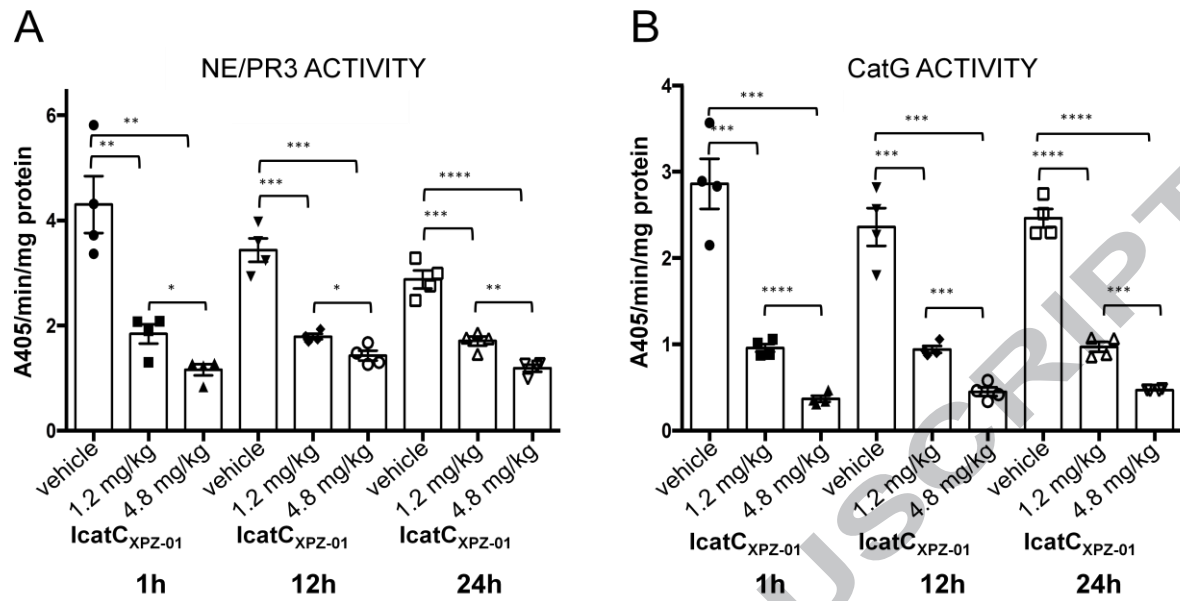


Compound 9a









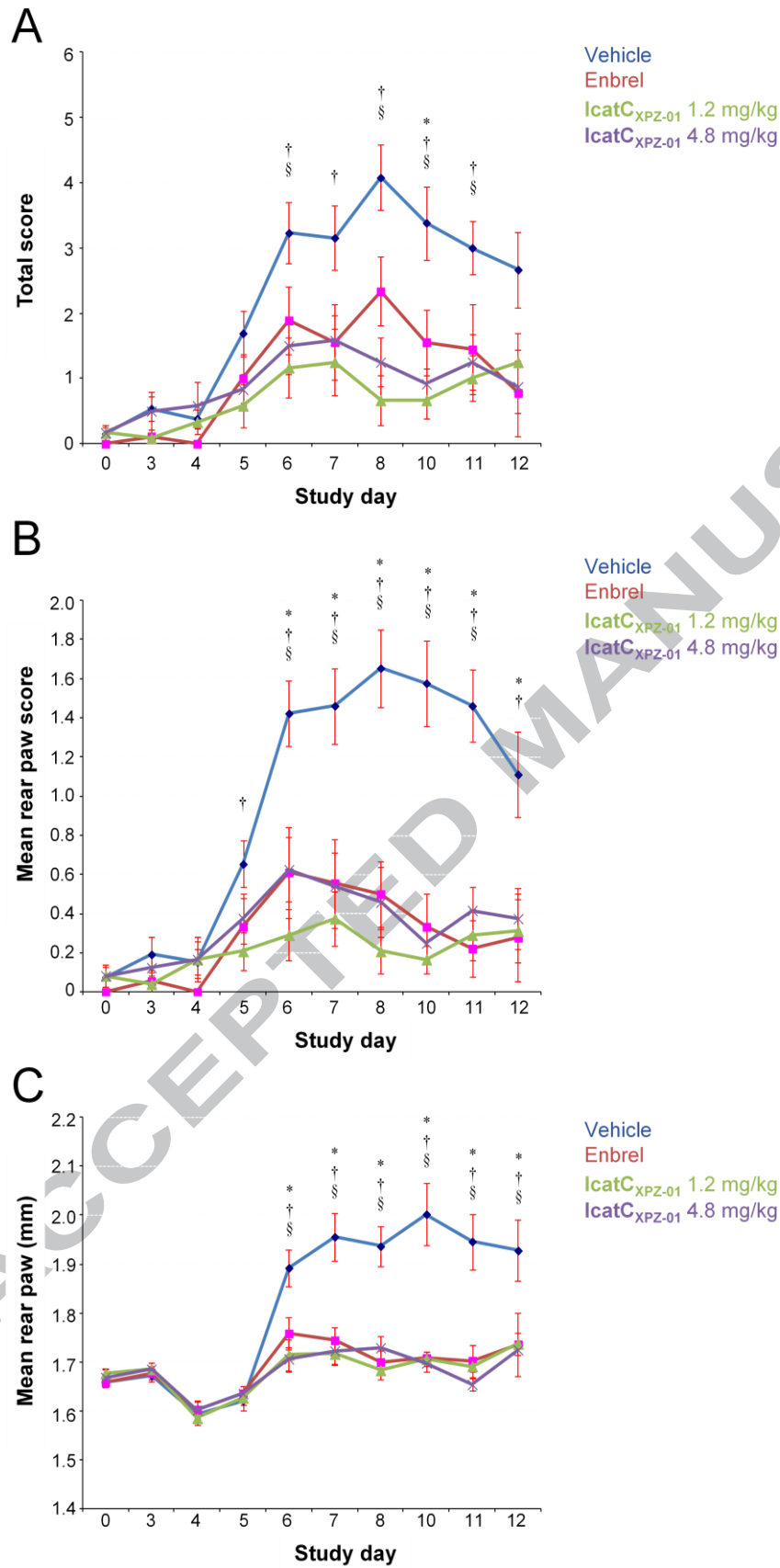


Table 1. Calculated and observed masses^a of synthesized inhibitors 1-14

Compound	Calculated mass (Da)	Found mass (Da)	
1	307.4	308.1	
2	325.5	326.1	
3	375.4	376.1	
		a	b
4	337.4	338.1	338.1
5	387.4	388.1	388.1
6	417.5	418.2	418.2
7	458.6	459.3	459.3
8	481.6	482.1	482.1
9	521.7	522.2	522.2
10	507.7	508.3	508.3
11	491.6	492.2	492.2
12	543.7	544.2	544.2
13	549.1	550.1	550.1
14	533.1	534.1	534.1

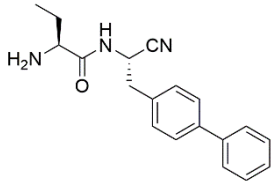
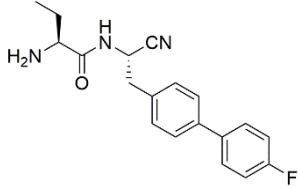
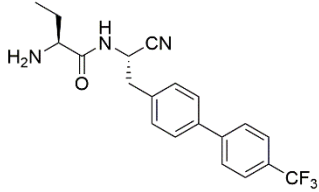
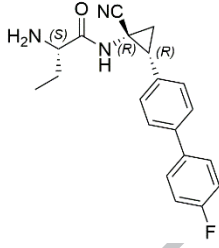
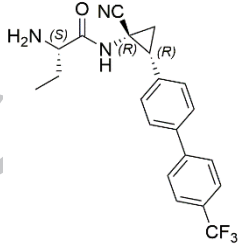
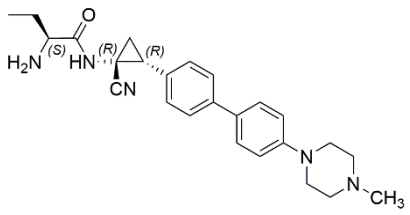
^aThe obtained molecular weights represent pseudomolar ions (M + H)⁺

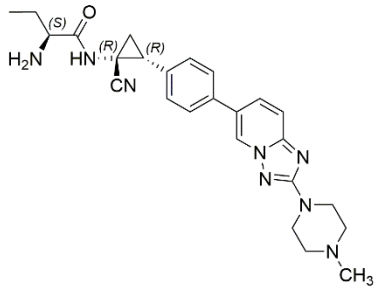
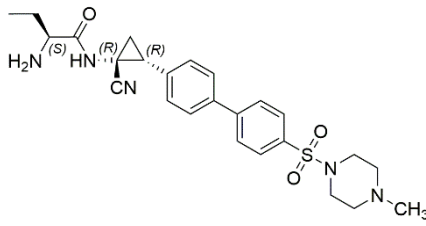
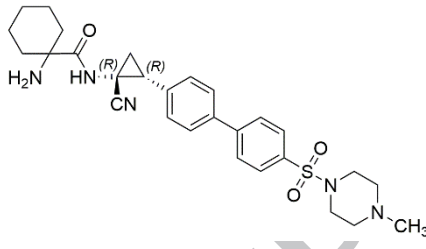
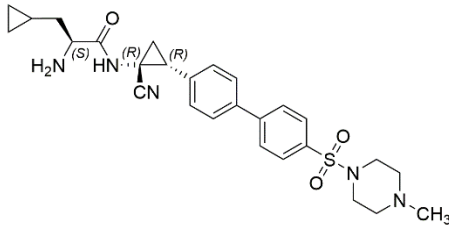
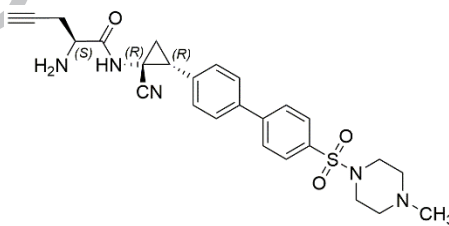
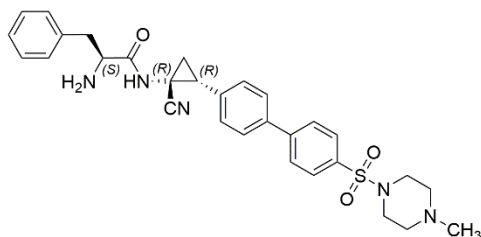
Table 2. Data collection and refinement statistics for inhibitor/CatC complexes

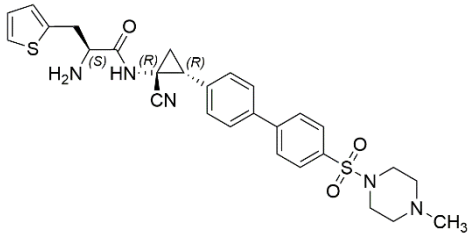
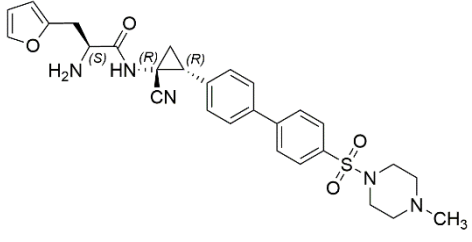
PDB ID codes	Compound		
	5a 6IC6	9a 6IC7	13a 6IC5
Data quality statistics			
Resolution (Å)	28.0-1.9 (1.95-1.9)	28.3-2.0 (2.1-2.0)	28.2-2.0 (2.1-2.0)
Wavelength (Å)	1.0412	1.5418	1.5418
Space group	I222	I222	I222
Unit cell	87.7 86.7 115.0	87.7 86.7 115.0	87.7 86.7 115.0
Completeness (%)	97.2 (96)	98.2 (85.5)	94.0 (61.2)
Average redundancy	3.7	11.5	11.9
No. of unique reflections	34042	30537	29396
$\langle I/\sigma(I) \rangle$	18.4 (3.4)	23.8 (6.1)	29.8 (6.9)
R _{merge} (I) (%)	5.0 (39.4)	6.9 (16.4)	6.0 (21.2)
Refinement quality statistics			
Resolution for refinement	28.0-1.9 (1.92-1.9)	27.5-2.0 (2.02-2.0)	28.2-2.0 (2.02-2.0)
R _{cryst} (F) (%)	14.7 (20.0)	15.3 (20.1)	16.0 (23.0)
R _{free} (F) (%)	18.6 (22.2)	20.2 (26.0)	20.3 (27.0)
No. of non-hydrogen atoms	3207	3279	3300
No. of water molecules	296	372	349
Root mean square (rms) deviations from ideal geometry:			
-bond lengths (Å)	0.014	0.012	0.014
-bond angles (°)	1.9	1.8	1.9
Median B-factor (protein, Å ²)	25	15	17
Median B-factor (ligand, Å ²)	33	19	20

Numbers in parentheses refer to the highest resolution shell.

Table 3. IC₅₀ values for compounds 1-14

Compound	Chemical structure / Name	IC ₅₀ CatC ^a (nM)	IC ₅₀ U937 ^a (nM)	Metabolic stability mouse microsomes t _{1/2} (min)
1		8.5 ^b	-	2
2		5.5	-	20
3		1.7	-	55
4a		18	110	41
4b		1060	-	-
5a		15	460	>60
5b		1390	-	-
6a		661	74	49
6b		860	-	-

7a		52	17	> 60
7b		≈1500	-	-
8a (IcatC _{XPZ-01})		15	6	11
8b		≈1500	-	-
9a		78	8	9
10a		89	25	31
10b		≈ 10.000	-	-
11a		17	16	40
11b		≈ 1500	-	-
12a		10	4	3

12b		≈1200	-	-
13a		6	0.75	2
13b		90	-	-
14a		5	1.5	2
14b		90	-	-

^aValues are the means \pm S.D of $n \geq 4$ experiments. For the sake of clarity, the errors attached to them are not given but are all lower than 20%.

^bIC₅₀ = 13 nM determined in Ref³¹.

Table 4: *In vitro* metabolic stabilities of cyclopropyl nitrile inhibitors in human and mouse liver microsomes

Species	Test compound	% Remaining of initial ^a					Half-Life (min)	CL _{int} ^c (mL/min/mg protein)	Metabolite detected ^d
		0 (min)	10	20	30	60			
Human	IcatC _{XPZ-01}	100	80.3	61.4	52.9	37.5	43	0.032	Yes
	compound 7a	100	91.1	80.7	79.6	77.7	>60 (178)	0.0078	Yes
	compound 12a	100	19.6	8.38	4.10	2.56	<10 (12)	0.11	Yes
	compound 13a	100	23	5.6	3.0	<1.0	4.8	0.29	Yes
Mouse	IcatC _{XPZ-01}	100	50	28	18	6.4	11	0.12	Yes
	compound 13a	100	5.5	1.7	1.5	1.0	2.4	0.58	Yes
	compound 14a	100	5.4	<1.0	<1.0	<1.0	2.4	0.58	Yes

^aPercent remaining of test compound was calculated based on the peak area ration of the test compound to the internal standard.

^bHalf-life was calculated based on half-life=0.693/k, where k is the elimination rate constant based on the slope of the plot of natural logarithm percent remaining versus incubation time.

^cIntrinsic clearance (CL_{int}) was calculated based on CL_{int}=k/P, where k is the elimination rate constant and P is the microsomal protein concentration in the incubation.

^dExpected metabolite detected.

The enzyme activities of human and mouse liver microsomes (0.5 mg/protein/mL) used in this study were verified in parallel by determining the disappearance of testosterone. The half-life of testosterone (positive control) demonstrated that testosterone was significantly metabolized, indicating that the human and mouse liver microsomes used in this study were metabolically active.

Table 5. *In vitro* profiling data for IcatC_{XPZ-01}

Human microsomal half-life, $t_{1/2}$ (min)	43
Mouse microsomal half-life, $t_{1/2}$ (min)	11
Human plasma stability $t_{1/2}$ (min)	>120
Mice plasma stability ($t_{1/2}$) (min)	>100 ^a
hERG IC ₅₀ (μM)	>25
CYP2C9 IC ₅₀ (μM)	>100
CYP2D6 IC ₅₀ (μM)	>100
CYP3A4 IC ₅₀ (μM)	>100
<i>CYP mRNA induction potential</i>	
<i>Fold induction</i>	
CYP1A2 induction – 1 μM	1.01
– 10 μM	1.01
CYP2B6 induction – 1 μM	1.03
– 10 μM	0.94
CYP3A4 induction – 1 μM	1.10
– 10 μM	1.06

^aEstimated

Table 6. Selected pharmacokinetic parameters and bioavailability for IcatC_{XPZ-01} after subcutaneous administration in mice at 4.8 mg/kg

	Single dose group (Group 1)	Two doses group (Group 2)
Pharmacokinetic parameter		
C _{max} (ng/mL)	758±82.1	342±17
t _{max} (h)	0.25	12.5
t _{1/2} (h)	3.0	43.5
AUC _{last} (±SE, h.ng/mL)	913±123	2115±100
AUC _∞ (±SE, h.ng/mL)	924	2200
Dose normalized parameters¹		
AUC _{last} (±SE, h.kg.ng/mL/mg)	190±25.6	441±20.8
AUC _∞ (±SE, h.kg.ng/mL/mg)	192	463
Bioavailability² (%)	78	-

Mice in group 2 received two separate subcutaneous doses of IcatC_{XPZ-01} (4.8 mg/kg) at time 0, and again at 12 h post 1st dose.

C_{max}: maximum plasma concentration; t_{max}: time of maximum plasma concentration; t_{1/2}: half-life; AUC_{last}: area under the curve, calculated to the last observable time point; AUC_∞: area under the curve, extrapolated to infinity;

¹Dose normalized by dividing the parameter by the dose in mg/kg;

²Bioavailability values are determined by dividing the SC AUC_∞ by the IV AUC_∞ from the pharmacokinetic study of IcatC_{XPZ-01}.